

Reactions of Aluminum, Gallium, and Indium (M) Atoms with Phosphine: Generation and Characterization of the Species $M\cdot PH_3$, $HMPH_2$, and H_2MPH

Hans-Jörg Himmel,* Anthony J. Downs, and Tim M. Greene

Inorganic Chemistry Laboratory, University of Oxford, South Parks Road, Oxford OX1 3QR, U.K.

Received July 25, 2000

Upon deposition of Al, Ga, or In atoms (M) together with phosphine in a solid argon matrix, metal atom complexes $M\cdot PH_3$ are formed. Photolysis of the matrices at $\lambda = 436$ nm results in the tautomerization of the adduct species to the insertion products $HMPH_2$ and H_2MPH . In addition, PH is formed from the reactions with Ga and In, with $HMPH_2$ being its most likely precursor. Further photolysis into the absorption maximum of $HMPH_2$ near 550 nm results in decomposition of $HMPH_2$ with partial re-formation of the adduct $M\cdot PH_3$ and further buildup of PH. H_2MPH is photostable under these conditions but suffers decomposition under the action of UV light ($200 \leq \lambda \leq 400$ nm). All the molecules have been identified by their IR spectra, the assignments being attested by the effects of deuteration and also by comparison either with the vibrational properties anticipated by density functional theory (DFT) calculations or with those of known, related molecules. The resulting analysis is elaborated for the light it sheds on the structures and properties of the new molecules and on the mechanisms of the reactions affording, or disposing of, them.

Introduction

Compounds featuring a bond between a group 13 and a group 15 element are notable mainly because of their potential use as precursors or intermediates in the chemical vapor deposition (CVD) formation of III–V semiconductor materials. AlP, GaP, and InP crystals have band gaps that are ideal for certain applications (2.45, 2.26, and 1.35 eV, respectively, at 300 K), and semiconductor devices based on GaP and InP are indeed in use in LEDs, long-wavelength IR sources, and detectors for optical fiber transmission.¹ Beyond this interest driven by industrial applications, the compounds attract attention for their potential to engage the group 13 and group 15 atoms together in multiple bonding.²

Matrix-isolation experiments have already contributed notably to the study of highly reactive phosphine derivatives.^{3–5} For example, insertion reactions of the main group atoms O and S into a P–H bond of PH_3 have been observed in this way to yield the products $HOPH_2$ ^{3,4} and $HSPH_2$,⁵ respectively. Complexes of PH_3 with transition metal atoms or compounds have also been characterized.^{6–8} Cocondensation of Cu atoms with PH_3 in Kr matrices results in the formation of $Cu(PH_3)_n$ complexes ($n = 1, 2, \text{ or } 3$)⁶ identified by IR absorptions at 2250 and 970, 968, and 958 cm^{-1} . Similar experiments indicate that Ni atoms add PH_3 to give $Ni(PH_3)$ or $Ni(PH_3)_4$ in Ar or neat

PH_3 matrices, respectively.^{6,7} The 1:1 complex $H_3P\cdot TiCl_4$ has also been characterized in this way.⁸

We have recently reported on the matrix reactions that occur between Al, Ga, or In atoms and NH_3 .⁹ The first product is a relatively well-defined adduct $M\cdot NH_3$ that tautomerizes to the insertion product $HMNH_2$ upon irradiation into its absorption maximum near 440 nm. Broad-band UV–visible photolysis then leads to the generation of the univalent metal amide MNH_2 , together with the trivalent derivative H_2MNH_2 . The IR spectra of the H_2MNH_2 molecules are wholly consistent with the results of density functional theory (DFT) calculations, which impute a planar geometry. However, the calculations find only small barriers to rotation (< 70 $kJ\ mol^{-1}$), indicating that π interactions play only a minor role in the bonding.⁹

Here we report on similar studies of the thermal and photochemical matrix reactions that occur between group 13 metal atoms and PH_3 . On the evidence of the IR and UV–vis spectra of the matrices, we shall show that the metal atoms in their ²P ground states form a loosely bound complex $M\cdot PH_3$ ($M = Al, Ga, \text{ or } In$) that is photolabile and rearranges on irradiation with light at wavelengths near 440 nm to yield two insertion products, namely, the M(II) species $HMPH_2$ and the M(III) species H_2MPH . PH is observed in addition, but only in the reactions of Ga and In, probably through the photodecay of $HMPH_2$. Photolysis at wavelengths near 546 nm causes decomposition of $HMPH_2$, while H_2MPH persists. UV irradiation ($200 \leq \lambda \leq 400$ nm) brings about the destruction of the H_2MPH derivatives. The identities of the products have been endorsed (i) by the response of the relevant IR absorptions to replacement of PH_3 by PD_3 , (ii) by comparison with the results of DFT calculations, and (iii) by reference to the vibrational properties of known, related molecules, e.g., $M\cdot NH_3$,⁹ HMX

* To whom correspondence should be addressed. Phone: 0044-1865-272673. Fax: 0044-1865-272690. E-mail: tony.downs@chem.ox.ac.uk.

- (1) Downs, A. J., Ed. *Chemistry of Aluminium, Gallium, Indium and Thallium*; Blackie: Glasgow, U.K., 1993. Edgar, J. H., Ed. *Properties of Group III Nitrides*; EMIS: London, U.K., 1994. Sze, S. M., Ed. *Physics of Semiconductor Devices*, 2nd ed.; Wiley: New York, 1981.
- (2) Power, P. P. *Chem. Rev.* **1999**, *99*, 3463. Cowley, A. H.; Jones, R. A. *Angew. Chem., Int. Ed. Engl.* **1989**, *28*, 1018.
- (3) Withnall, R.; Andrews, L. *J. Phys. Chem.* **1987**, *91*, 784.
- (4) Withnall, R.; Andrews, L. *J. Phys. Chem.* **1988**, *92*, 4610.
- (5) Mielke, Z.; Andrews, L. *J. Phys. Chem.* **1993**, *97*, 4313.
- (6) Bowmaker, G. A. *Aust. J. Chem.* **1978**, *31*, 2549.
- (7) Trabelsi, M.; Loutellier, A. *J. Mol. Struct.* **1978**, *43*, 151.
- (8) Everhart, J. B.; Ault, B. S. *Inorg. Chem.* **1996**, *35*, 4090.

(9) Himmel, H.-J.; Downs, A. J.; Greene, T. M. *J. Chem. Soc., Chem. Commun.* **2000**, 871. Himmel, H.-J.; Downs, A. J.; Greene, T. M. *J. Am. Chem. Soc.* **2000**, *122*, 9793.

(X = H,¹⁰ OH,¹¹ CH₃,^{12,13} or NH₂⁹), and H₂MX (X = H,¹⁴ Cl,¹⁵ or NH₂⁹). The properties observed or forecast for M·PH₃, HMPH₂, and H₂MPH will be compared with those of analogous group 13 metal derivatives, particularly M·NH₃ and HMNH₂,⁹ and discussed in relation to the characters of the relevant bonds.

Experimental Section

Aluminum (Aldrich, purity 99.999%), gallium (Aldrich, purity 99.9999%), and indium (Aldrich, purity 99.999%) were each evaporated from a tantalum Knudsen cell that was heated resistively to ca. 1000 °C for Al and 900 °C for Ga and In. Hence the metal vapor was codeposited with an excess of PH₃-doped argon on a CsI window cooled normally to ca. 12 K by means of a Displex closed-cycle refrigerator (Air Products, model CS202). Fuller details of the matrix apparatus are given elsewhere.^{9,13} The estimated proportions M/PH₃/Ar (M = Al, Ga, or In) were typically in the order 1:10:600. Normal deposition rates were ca. 2 mmol of matrix gas per hour, continued over a period of 2–3 h. Similar experiments were carried out with PD₃ in place of PH₃.

PH₃ and PD₃ were synthesized starting from calcium phosphide and either H₂O or D₂O and purified by fractional condensation in vacuo. Argon was used as received from BOC (Research grade purity). Gas mixtures of argon with PH₃ or PD₃ were prepared by standard manometric methods.

After deposition and IR or UV–vis analysis of the resulting matrix, the sample was exposed first to visible radiation with $\lambda \approx 436$ nm. Once the effects of such photolysis had been assessed, the sample was typically irradiated in turn with visible light at $\lambda \approx 546$ nm and finally with broad-band UV–visible light with $\lambda = 200$ –800 nm. The photolyzing radiation issuing from a Spectral Energy HgXe arc lamp operating at 800 W was invariably limited by a water filter to absorb infrared radiation and so minimize any heating effects. Visible radiation with $\lambda \approx 436$ or 546 nm and a band-pass of 20 nm was delivered via an appropriate interference filter (Balzers).

IR spectra of the matrix samples were recorded, typically at a resolution of 0.5 cm⁻¹ and with an accuracy of ± 0.1 cm⁻¹, using a Nicolet Magna-IR 560 FTIR spectrometer equipped with a liquid-N₂-cooled MCTB or with a DTGS detector (for the ranges 4000–400 or 600–200 cm⁻¹, respectively). UV–vis spectra were recorded in the range 300–900 nm using a Perkin-Elmer-Hitachi model 330 spectrophotometer.

Density functional theory (DFT) calculations were performed using the Gaussian 98 program package¹⁶ and applying the B3LYP method, which has been shown to give satisfactory results for small aluminum and gallium compounds.¹⁷ A 6-311G(d) basis set was used for Al and

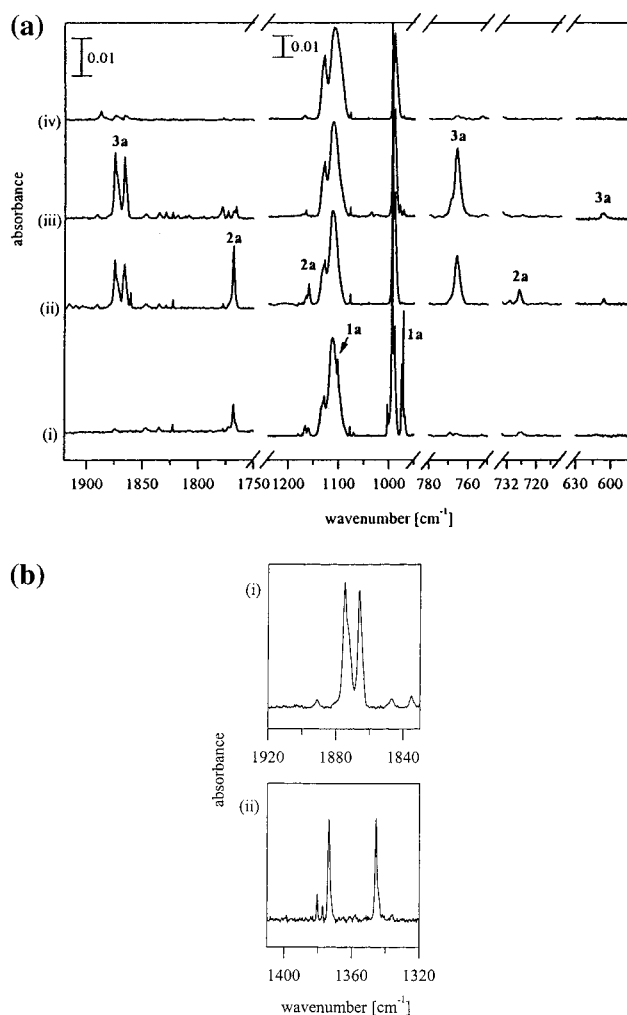


Figure 1. (a) IR spectra of an Ar matrix containing Al and PH₃ (1.5%): (i) following deposition; (ii) following photolysis at $\lambda = 436$ nm; (iii) following photolysis at $\lambda = 546$ nm; (iv) following broad-band UV–visible photolysis ($\lambda = 200$ –800 nm). (b) IR spectra of Ar matrices after 546 nm photolysis showing the signals at 1874.7/1866.1 and 1373.5/1345.6 cm⁻¹ due to product **3a** as formed from (i) PH₃ and (ii) PD₃, respectively.

Ga, and a LANL2DZ basis set with additional d-polarization functions (exponent of 0.5) was used for In. All the vibrational frequencies calculated for the optimum geometries and cited hereafter are unscaled.

Results

The spectra associated with the matrix-isolated products of the reactions of phosphine with group 13 metal atoms (M) will be reported in turn for M = Al, Ga, and In. Products have been identified on the basis of (i) the growth and decay characteristics of the relevant spectroscopic features in response to photolysis of the matrix under different conditions or to changes of reagent concentration, and (ii) comparisons with the results of control experiments that did not include the metal atoms, or with the spectra of related species.

(i) Al + PH₃. Figure 1 displays the IR spectra of an argon matrix containing ca. 0.2% Al atoms and 1.5% PH₃ before and after irradiation under various conditions; details of the spectra are itemized in Table 1. Following deposition, the IR spectrum witnessed, in addition to the signals due to PH₃ (at 2344.7, 2339.1, 1111.7, and 993.7 cm⁻¹),¹⁸ [PH₃]_n (low-frequency

- (10) Pullumbi, P.; Mijoule, C.; Manceron, L.; Bouteiller, Y. *Chem. Phys.* **1994**, *185*, 13.
- (11) Hauge, R. H.; Kauffman, J. W.; Margrave, J. L. *J. Am. Chem. Soc.* **1980**, *102*, 6005.
- (12) Parnis, J. M.; Ozin, G. A. *J. Phys. Chem.* **1989**, *93*, 1204, 1220. Lafleur, R. D.; Parnis, J. M. *J. Phys. Chem.* **1992**, *96*, 2429.
- (13) Himmel, H.-J.; Downs, A. J.; Greene, T. M.; Andrews, L. *J. Chem. Soc., Chem. Commun.* **1999**, 2243. Himmel, H.-J.; Downs, A. J.; Greene, T. M.; Andrews, L. *Organometallics* **2000**, *19*, 1060.
- (14) Pullumbi, P.; Bouteiller, Y.; Manceron, L.; Mijoule, C. *Chem. Phys.* **1994**, *185*, 25.
- (15) (a) Himmel, H.-J.; Downs, A. J.; Greene, T. M. *J. Am. Chem. Soc.* **2000**, *122*, 922. (b) Köppe, R.; Schnöckel, H. *J. Chem. Soc., Dalton Trans.* **1992**, 3393.
- (16) Frisch, M. J.; Trucks, G. W.; Schlegel, H. B.; Scuseria, G. E.; Robb, M. A.; Cheeseman, J. R.; Zakrzewski, V. G.; Montgomery, J. A., Jr.; Stratmann, R. E.; Burant, J. C.; Dapprich, S.; Millam, J. M.; Daniels, A. D.; Kudin, K. N.; Strain, M. C.; Farkas, O.; Tomasi, J.; Barone, V.; Cossi, M.; Cammi, R.; Mennucci, B.; Pomelli, C.; Adamo, C.; Clifford, S.; Ochterski, J.; Petersson, G. A.; Ayala, P. Y.; Cui, Q.; Morokuma, K.; Malick, D. K.; Rabuck, A. D.; Raghavachari, K.; Foresman, J. B.; Cioslowski, J.; Ortiz, J. V.; Stefanov, B. B.; Liu, G.; Liashenko, A.; Piskorz, P.; Komaromi, I.; Gomperts, R.; Martin, R. L.; Fox, D. J.; Keith, T.; Al-Laham, M. A.; Peng, C. Y.; Nanayakkara, A.; Gonzalez, C.; Challacombe, M.; Gill, P. M. W.; Johnson, B. G.; Chen, W.; Wong, M. W.; Andres, J. L.; Head-Gordon, M.; Replogle, E. S.; Pople, J. A. *Gaussian 98*, revision A.3; Gaussian, Inc.: Pittsburgh, PA, 1998.

(17) Jursic, B. S. *J. Mol. Struct.: THEOCHEM* **1998**, *428*, 61.

(18) Arlinghaus, R. T.; Andrews, L. *J. Chem. Phys.* **1984**, *81*, 4341.

Table 1. Infrared Absorptions (Frequencies in cm^{-1}) Displayed by Ar Matrices Containing Al Atoms and PH_3/PD_3

Al + PH_3	Al + PD_3	deposition ^a	λ^a (nm)			absorber
			436	546	200–800	
2285.5	1659.4	↑	↓	↑	↓	$\text{Al}\cdot\text{PH}_3$, 1a
1874.7	1373.5		↑	↑	↓	H_2AlPH , 3a
1867.4	<i>b</i>		↑	↓	↓	$\text{H}_2\text{AlPH}\cdot\text{PH}_3$
1866.1	1345.6		↑	↑	↓	H_2AlPH , 3a
1860.6	<i>b</i>		↑	↑	↓	$\text{H}_2\text{AlPH}\cdot\text{PH}_3$
1768.2	1288.4	↑	↑	↓	↓	HAIPH_2 , 2a
1159.4	<i>b</i>	↑	↑	↓	↓	HAIPH_2 , 2a
1101.2	793.7	↑	↓	↑	↓	$\text{Al}\cdot\text{PH}_3$, 1a
974.7	718.3	↑	↓	↑	↓	$\text{Al}\cdot\text{PH}_3$, 1a
971.2	717.0	↑	↓	↓	↓	$\text{Al}\cdot(\text{PH}_3)_2$
765.9	564.5		↑	↑	↓	H_2AlPH , 3a
727.1	532.3	↑	↑	↓	↓	HAIPH_2 , 2a
606.3	482.8		↑	↑	↓	H_2AlPH , 3a
569.0	<i>b</i>		↑	↑	↓	H_2AlPH , 3a
403.9	<i>b</i>	↑	↑	↓	↓	HAIPH_2 , 2a

^a ↑: increase. ↓: decrease. ^b Too weak to be detected or hidden by PH_3 absorptions.

shoulders on the signals due to monomeric PH_3 ,¹⁸ H_2O , and $[\text{H}_2\text{O}]_n$,¹⁹ the appearance of a strong signal at 974.7 cm^{-1} . Correlating with this feature were a sharp signal at 1101.2 cm^{-1} and another at higher frequency, viz. 2285.5 cm^{-1} . The three bands are attributable to the first reaction product, **1a**. The spectrum also contained a weak absorption at 1002.8 cm^{-1} , belonging in all probability to a repulsive PH_3 site, as well as a band at 971.2 cm^{-1} and an additional family of weak bands belonging to a common species **2a**, these being located at 1768.2 , 1159.4 , 727.1 , and 403.9 cm^{-1} .

Upon photolysis with radiation at $\lambda \approx 436\text{ nm}$ for a period of 5 min, the signals due to **1a** disappeared and the bands due to **2a** were observed to grow. The strongest feature of **2a** occurs at a frequency (1768.2 cm^{-1}) close to that of the $\nu(\text{Al}-\text{H})$ stretching mode in known divalent aluminum hydrides (AlH_2 $1806.3/1769.5$,¹⁰ HAIOH 1739.6 ,¹¹ CH_3AlH $1764/1746$,¹² and HAlNH_2 1761.1 cm^{-1}).⁹ In addition, the spectrum revealed a new family of absorptions with frequencies of 1874.7 , 1866.1 , 765.9 , 606.3 , and 569.0 cm^{-1} originating in yet a third and distinct product, **3a**. The high-frequency bands at 1874.7 and 1866.1 cm^{-1} are significant in that they occur in the region normally associated with the $\nu(\text{Al}-\text{H})$ frequencies of terminal $\text{Al}(\text{III})-\text{H}$ bonds (cf. AlH_3 1882.9 cm^{-1} ,¹⁴ HAICl_2 1967.6 cm^{-1} ,²⁰ $[\text{H}_2\text{AlNMe}_2]_3$ $1800-1850\text{ cm}^{-1}$,²¹ and H_2AlNH_2 1899.3 cm^{-1}). A weak doublet feature also developed at $1867.4/1860.6\text{ cm}^{-1}$.

There followed a period (5 min) of irradiation at $\lambda \approx 546\text{ nm}$. This caused the signals due to species **2a** to vanish and those due to **1a** to regain some of the intensity they had prior to photolysis. Simultaneously the doublet at $1867.4/1860.6\text{ cm}^{-1}$ disappeared. Finally, the matrix was exposed either to broad-band UV radiation ($\lambda = 200-400\text{ nm}$) or to broad-band UV-visible radiation ($\lambda = 200-800\text{ nm}$). In either case the IR bands associated with **3a** vanished without the appearance of any significant features in the region $200-4000\text{ cm}^{-1}$ attributable to a new product.

The experiment was repeated but with PD_3 in place of PH_3 . Upon deposition, the matrix displayed IR absorptions due to **1a** but now shifted to substantially lower frequency. Thus, the

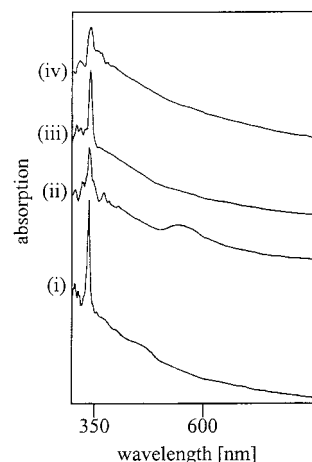


Figure 2. UV-vis spectra (a) of an Ar matrix containing Al and (b) of an Ar matrix containing Al and PH_3 : (i) following deposition; (ii) following photolysis at $\lambda = 436\text{ nm}$; (iii) following photolysis at $\lambda = 546\text{ nm}$; (iv) following broad-band UV-visible photolysis ($\lambda = 200-800\text{ nm}$).

signal at 974.7 cm^{-1} gave place to one at 718.3 cm^{-1} ($\text{H/D} = 1.3570:1$), while the bands at 2285.5 and 1101.2 cm^{-1} shifted to 1659.4 ($\text{H/D} = 1.3773:1$) and 793.7 cm^{-1} ($\text{H/D} = 1.3874:1$), respectively. The weak band at 1002.8 cm^{-1} observed in the earlier spectrum appeared to have a counterpart at 738.9 cm^{-1} ($\text{H/D} = 1.3572:1$) in the PD_3 experiment. The signal at 971.2 cm^{-1} moved to 717.0 cm^{-1} ($\text{H/D} = 1.3545:1$).

The prominent transition at 1768.2 cm^{-1} due to the PH_3 version of species **2a** shifted to 1288.4 cm^{-1} ($\text{H/D} = 1.3724:1$), whereas the transition at 727.1 cm^{-1} shifted to 532.3 cm^{-1} ($\text{H/D} = 1.3660:1$). No counterparts to the weak bands at 1159.4 and 403.9 cm^{-1} could be detected before or after photolysis at 436 nm . On the other hand, four absorptions attributable to the deuterated version of **3a** were observed. Hence, it appeared that the 1874.7 cm^{-1} transition moved to 1373.5 cm^{-1} ($\text{H/D} = 1.3649:1$), the 1866.1 cm^{-1} transition to 1345.6 cm^{-1} ($\text{H/D} = 1.3868:1$), the 765.9 cm^{-1} transition to 564.5 cm^{-1} ($\text{H/D} = 1.3568:1$), and the 644.5 cm^{-1} transition to 482.8 cm^{-1} ($\text{H/D} = 1.3349:1$).

In another experiment the concentration of PH_3 was reduced to 0.5%. All the IR signals observed in the experiments with higher concentrations were also observed in this case but with lower intensities. However, the relative intensities of the absorptions belonging to each of the species **1a-3a** remained unchanged. The feature at 974.7 cm^{-1} (due to **1a**) gained in intensity at the expense of the neighboring one at 971.2 cm^{-1} . By contrast, the intensity of the doublet at $1867.4/1860.6\text{ cm}^{-1}$ dropped significantly relative to those of the signals due to **1a-3a**.

Experiments in which the matrix was photolyzed immediately after deposition either with UV radiation ($200 \leq \lambda \leq 400\text{ nm}$) or with radiation at $\lambda \geq 450\text{ nm}$ led to the disappearance of the bands due to **1a** and **2a** without any sign of additional products (except for very weak bands due to **3a**, which is presumably formed in consequence of photolysis into the long tail of the $\text{Al}\cdot\text{PH}_3$ absorption). Further experiments were carried out using mixtures of PH_3 and H_2 . However, the addition of H_2 did not lead to significant changes in the relative intensities of the bands associated with **1a-3a**.

Figure 2 illustrates the UV-vis spectra measured over the range $300-900\text{ nm}$ for an argon matrix doped with Al atoms and PH_3 . The spectrum recorded after deposition shows a sharp absorption at 337 nm , which has previously been assigned to

(19) Greene, T. M.; Andrews, L.; Downs, A. J. *J. Am. Chem. Soc.* **1995**, *117*, 8180.

(20) Schnöckel, H. J. *Mol. Struct.* **1978**, *50*, 275.

(21) Downs, A. J.; Duckworth, D.; Machell, J. C.; Pulham, C. R. *Polyhedron* **1992**, *11*, 1295.

Table 2. Infrared Absorptions (Frequencies in cm^{-1}) Displayed by Ar Matrices Containing Ga Atoms and PH_3/PD_3

Ga + PH_3	Ga + PD_3	deposition ^a	λ^a (nm)			absorber
			436	546	200–800	
2280.8	1660.3	↑	↓	↑	↓	$\text{Ga}\cdot\text{PH}_3$, 1b
2248.9	1641.3		↑	↑	↓	PH
1918.4	<i>b</i>		↑	↓	↓	$\text{H}_2\text{GaPH}\cdot\text{PH}_3$
1913.2	<i>b</i>		↑	↓	↓	$\text{H}_2\text{GaPH}\cdot\text{PH}_3$
1897.5	1372.8		↑	↑	↓	H_2GaPH , 3b
1893.3	1360.1		↑	↑	↓	H_2GaPH , 3b
1721.4	1244.7	↑	↑	↓	↓	HGaPH_2 , 2b
1108.2	795.9	↑	↓	↑	↓	$\text{Ga}\cdot\text{PH}_3$, 1b
1060.9	<i>b</i>	↑	↑	↓	↓	HGaPH_2 , 2b
973.6	717.7	↑	↓	↑	↓	$\text{Ga}\cdot\text{PH}_3$, 1b
969.3	714.3	↑	↓	↓	↓	$\text{Ga}\cdot(\text{PH}_3)_2$
738.9	528.8		↑	↑	↓	H_2GaPH , 3b
646.5/644.8	486.4		↑	↑	↓	H_2GaPH , 3b
454.8	<i>b</i>		↑	↑	↓	H_2GaPH , 3b
428.2	<i>b</i>	↑	↑	↓	↓	HGaPH_2 , 2b

^a ↑: increase. ↓: decrease. *b* Too weak to be detected or hidden by PH_3 absorptions.

the $2\text{S} \leftarrow 2\text{P}$ transition of Al atoms.^{9,22} No other feature could be detected with any certainty. Upon photolysis at wavelengths near 436 nm, the 337 nm absorption decreased and a new, broad signal with its maximum at 550 nm appeared [spectrum ii of Figure 2]. At the same time, the IR spectrum witnessed the appearance of the bands characteristic of **2a**. Thus, the absorption at 550 nm is presumed to be carried by the same species **2a**. Photolysis at wavelengths near 550 nm or with UV radiation ($\lambda = 200\text{--}400$ nm) led to the decay of the 550 nm absorption with no sign of any new feature. The absorption arising from the Al atoms did not obviously regain any of its initial intensity.

(ii) **Ga + PH_3 .** Figure 3 depicts the IR spectra displayed by an argon matrix containing ca. 0.2% Ga atoms and 1.5% PH_3 before and after photolysis; details of the spectra are itemized in Table 2. Upon deposition, the matrix showed a strong absorption at 973.6 cm^{-1} , with additional features from the same source at 1108.2 and 2280.8 cm^{-1} . The frequencies and circumstances give every reason to believe that the carrier of these bands is an adduct **1b** analogous to the product **1a** formed in the corresponding reaction with Al atoms. An additional signal was observed at 969.3 cm^{-1} .

Upon photolysis of the matrix with radiation at $\lambda = \text{ca. } 436$ nm, the IR absorptions characterizing **1b** decreased and another set of absorptions, belonging to a species **2b** and with frequencies of 1721.4, 1060.9, and 428.2 cm^{-1} , were observed to develop. These bands were already visible upon deposition but with very low intensities. The strong band at 1721.4 cm^{-1} is suggestively close in frequency to the $\nu(\text{Ga}\text{--}\text{H})$ stretching modes of known divalent gallium hydrides (GaH_2 $1799.5/1727.7\text{ cm}^{-1}$,¹⁰ CH_3GaH 1719.7 cm^{-1} ,¹³ HGaNH_2 1721.8 cm^{-1} ,⁹ and HGaOH 1669.8 cm^{-1} ¹¹). A weak doublet that appeared at $1918.4/1913.2\text{ cm}^{-1}$ but showed a rather different growth pattern was attributed to a distinct secondary product. Simultaneously a second family of five signals at 1897.5, 1893.3, 738.9, 646.5/644.8, and 454.8 cm^{-1} was observed to grow in, and this we associate with the distinct species **3b**. The transitions at 1897.5 and 1893.3 cm^{-1} occur in a region characteristic of the stretching vibrations of terminal $\text{Ga(III)}\text{--}\text{H}$ bonds, and that at 738.9 cm^{-1} likewise has the frequency and intensity characteristic of a GaH_2 deformation mode in a trivalent gallane derivative (cf. GaH_3 1923.2 and 758.7 cm^{-1} ,¹⁴ H_2GaCl $1964.6/1978.1$ and 731.4 cm^{-1} ,^{15b} $\text{H}_2\text{Ga}(\mu\text{--}\text{Cl})_2\text{GaH}_2$ $1994/2036$ and $702/719\text{ cm}^{-1}$,²³ $\text{H}_2\text{--}\text{Ga}(\mu\text{--}\text{H})_2\text{BH}_2$ $1982/2005$ and 729 cm^{-1} ,²⁴ and H_2GaNH_2 1970.8

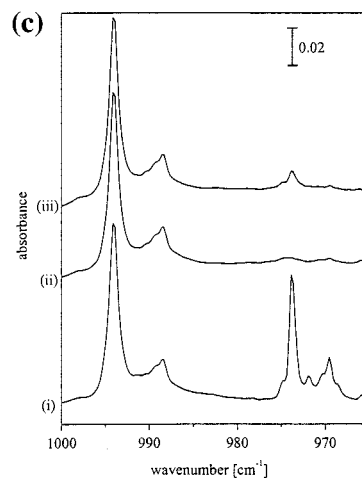
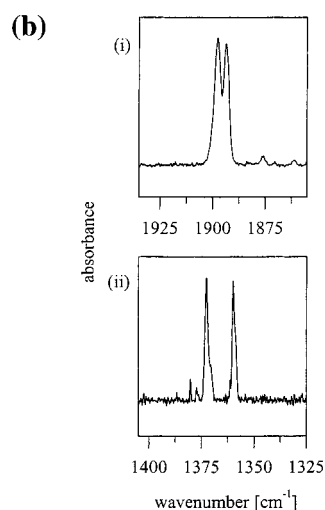
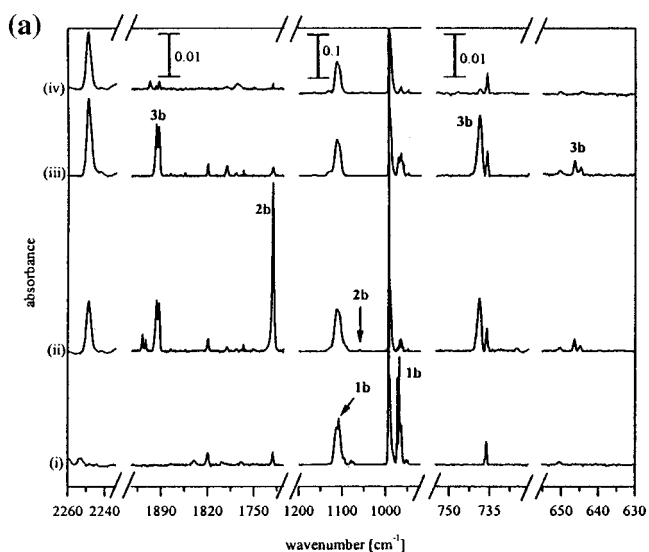


Figure 3. (a) IR spectra of an Ar matrix containing Ga and PH_3 (1.5%): (i) following deposition; (ii) following photolysis at $\lambda = 436$ nm; (iii) following photolysis at $\lambda = 546$ nm; (iv) following broadband UV–visible photolysis ($\lambda = 200\text{--}800$ nm). (b) IR spectra of Ar matrices after 546 nm photolysis, showing the signals at $1897.5/1893.3$ and $1372.8/1360.1\text{ cm}^{-1}$ due to product **3b** as formed from (i) PH_3 and (ii) PD_3 , respectively. (c) IR spectra of an Ar matrix containing Ga and PH_3 (0.4%) in the region $960\text{--}1000\text{ cm}^{-1}$ showing the features characteristic of the product **1b**: (i) following deposition; (ii) following photolysis at $\lambda = 436$ nm; (iii) following photolysis at $\lambda = 546$ nm.

and 779.6 cm^{-1}). In addition to the bands signaling the formation of **2b** and **3b**, there appeared a sharp band at 2248.9 cm^{-1} that found no equivalent in the experiments with Al atoms.

Following photolysis at wavelengths near 550 nm , the IR signals due to species **2b** disappeared while those due to **3b** persisted. The feature at 2248.9 cm^{-1} appeared to grow slightly. Broad-band UV photolysis ($200 \leq \lambda \leq 400\text{ nm}$) resulted, on the other hand, in the decay of the absorptions associated with **3b**, whereas the 2248.9 cm^{-1} absorption was observed to persist.

Experiments with PD_3 in place of PH_3 showed on deposition IR signs of the deuterated version of the species **1b** at 1660.3 ($\text{H/D} = 1.3737:1$), 795.9 ($\text{H/D} = 1.3924:1$), and, carrying most of the intensity, 717.7 cm^{-1} ($\text{H/D} = 1.3566:1$). The signal at 969.3 cm^{-1} shifted to 714.3 cm^{-1} ($\text{H/D} = 1.3570:1$). As noted in the experiments with PH_3 , these signals decreased sharply upon photolysis at $\lambda \approx 436\text{ nm}$, to be replaced by a signal at 1244.7 cm^{-1} ($\text{H/D} = 1.3830:1$) corresponding to the deuterated version of **2b** and four signals at 1372.8 ($\text{H/D} = 1.3822:1$), 1360.1 ($\text{H/D} = 1.3920:1$), 528.8 ($\text{H/D} = 1.3973:1$), and 486.4 cm^{-1} ($\text{H/D} = 1.3292:1$) corresponding to the deuterated version of **3b**. In addition, a signal at 1641.3 cm^{-1} that also developed at this stage can be traced to the deuterated version of the species responsible for the 2248.9 cm^{-1} absorption ($\text{H/D} = 1.3420:1$).

Experiments with lower PH_3 concentrations revealed no new features. All the signals assigned to species **1b–3b** were observed but with reduced intensities. The constant relative intensities of the bands belonging to each species confirm our recognition of the three principal products. On the other hand, the intensity of the doublet feature at $1918.4/1913.2\text{ cm}^{-1}$ decreased significantly relative to those of the signals due to the species **1b–3b**. Experiments in which the matrices were photolyzed immediately after deposition with either UV ($200 \leq \lambda \leq 400\text{ nm}$) or with $\lambda \geq 450\text{ nm}$ radiation resulted in the decay of the signals due to **1b** and the very weak ones due to **2b**. The signal that was observed to grow in at 2248.9 cm^{-1} was then the only sign of a reaction product (except for very weak bands due to **3b**, which is presumably formed as a consequence of photolysis into the long tail of the $\text{Ga}\cdot\text{PH}_3$ absorption).

(iii) In + PH₃. Following deposition of In atoms together with PH_3 in an argon matrix, a strong IR band at 974.4 cm^{-1} and a weaker one at 1105.7 cm^{-1} appeared in addition to those characteristic of PH_3 and $[\text{PH}_3]_n$, $^{18}\text{H}_2\text{O}$ and $[\text{H}_2\text{O}]_n$,¹⁹ and the water adduct $\text{H}_2\text{O}\cdot\text{In}$.^{9,11} These new signals are attributable to **1c**, the indium analogue of **1a** and **1b**. An additional signal was spotted at 968.0 cm^{-1} .

The absorptions of **1c** decreased rapidly upon photolysis at $\lambda \approx 436\text{ nm}$. At the same time, a new absorption at 1546.4 cm^{-1} with a weaker one at 2299.4 cm^{-1} , both belonging to species **2c**, were seen to evolve. An additional weak feature at 674.7 cm^{-1} could be tentatively assigned to **3c**, i.e., the indium analogue of **3a** and **3b**. As with the photochemical reactions initiated between Ga atoms and PH_3 , a new band at 2248.9 cm^{-1} also emerged at this stage. The response of the matrix to further photolysis was similar to that described for the experiments with Al and Ga atoms, **2c** being destroyed by visible light at $\lambda \approx 546\text{ nm}$ and both **2c** and **3c** being destroyed by UV light ($\lambda = 200\text{--}400\text{ nm}$), but no new band being discernible in the region $200\text{--}4000\text{ cm}^{-1}$. The signal at 2248.9 cm^{-1} grew somewhat on photolysis at $\lambda \approx 546\text{ nm}$ and persisted on UV photolysis.

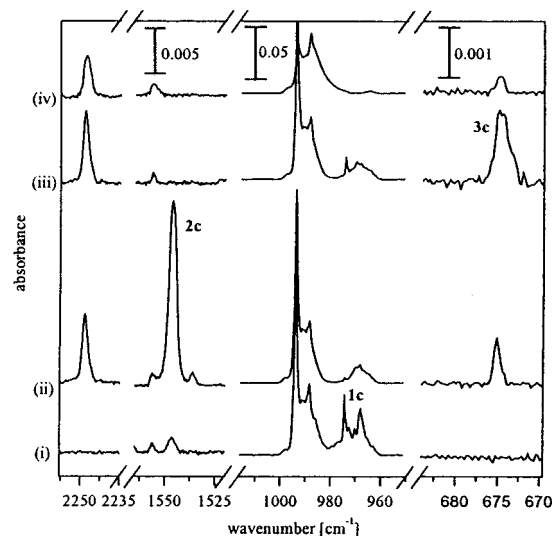


Figure 4. IR spectra of an Ar matrix containing In and PH_3 (1.5%): (i) following deposition; (ii) following photolysis at $\lambda = 436\text{ nm}$; (iii) following photolysis at $\lambda = 546\text{ nm}$; (iv) following broad-band UV-visible photolysis ($\lambda = 200\text{--}800\text{ nm}$).

Table 3. Infrared Absorptions (Frequencies in cm^{-1}) Displayed by Ar Matrices Containing In Atoms and PH_3/PD_3

In + PH_3	In + PD_3	deposition ^a	λ^a (nm)			absorber
			436	546	200–800	
2299.4	<i>b</i>	↑	↑	↓	↓	HInPH_2 , 2c
2248.9	1641.3	↑	↑	↑		PH
1546.4	1114.9	↑	↑	↓	↓	HInPH_2 , 2c
1105.7	<i>b</i>	↑	↓	↑	↓	$\text{In}\cdot\text{PH}_3$, 1c
974.4	717.6	↑	↓	↑	↓	$\text{In}\cdot\text{PH}_3$, 1c
968.0	713.2	↑	↓	↓	↓	$\text{In}\cdot(\text{PH}_3)_2$
674.7	<i>b</i>		↑	↑	↓	H_2InPH , 3c

^a ↑: increase. ↓: decrease. *b* Too weak to be detected or hidden by PH_3 absorptions.

Relevant IR spectra are illustrated in Figure 4; details of the spectra are listed in Table 3.

In the corresponding experiments with PD_3 , the IR signal at 974.4 cm^{-1} characteristic of the species **1c** shifted, as expected, to lower frequency (717.6 ; $\text{H/D} = 1.3579:1$), although no other feature identifiable with deuterated **1c** could be traced. The signal at 968.0 cm^{-1} shifted to 713.2 cm^{-1} ($\text{H/D} = 1.3573:1$). Photolysis at wavelengths near 436 nm brought about the decay of the signals at 717.6 and 713.2 cm^{-1} with the simultaneous appearance of a new weak band at 1114.9 cm^{-1} , which may be presumed to arise from the deuterated version of species **2c** and to correlate with the 1546.4 cm^{-1} transition of **2c** ($\text{H/D} = 1.3870:1$). Certainly its carrier showed the appropriate photochemical properties by decaying when the matrix was irradiated at wavelengths near 546 nm or in the range $200\text{--}400\text{ nm}$. Unfortunately it was not possible to locate any spectroscopic signs of the deuterated version of **3c**. Indeed, it appeared to be a general feature of the indium experiments that all the IR absorptions attributable to photoproducts were significantly weaker than were their counterparts in the aluminum and gallium experiments. Whether this reflects inherent weakness of the relevant transitions in IR absorption or, as seems more likely, low abundances of the products **2c** and **3c** remains to be seen.

As in the experiments with Ga, the signal at 2248.9 cm^{-1} was observed to grow in when the matrices were exposed to UV ($200 \leq \lambda \leq 400\text{ nm}$) or $\lambda \geq 450\text{ nm}$ radiation following deposition. But these experiments gave no sign of any other reaction product.

(23) Johnsen, E.; Downs, A. J.; Greene, T. M.; Souter, P. F.; Aarset, K.; Page, E. M.; Rice, D. A.; Richardson, A. N.; Brain, P. T.; Rankin, D. W. H.; Pulham, C. R. *Inorg. Chem.* **2000**, *39*, 719.

(24) Pulham, C. R. D.Phil. Thesis, University of Oxford, U.K., 1991.

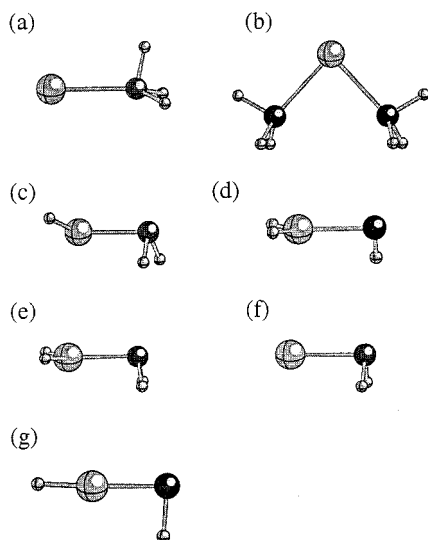


Figure 5. Calculated geometries of the molecules (a) $M\cdot PH_3$, (b) $M\cdot (PH_3)_2$, (c) $HMPH_2$, (d) H_2MPH , (e) H_2MPH_2 , (f) MPH_2 , and (g) $HMPH$ ($M = Al, Ga, \text{ or } In$).

Discussion

Here we shall show that the products **1a–c** are adducts of the type $M\cdot PH_3$, that **2a–c** are the divalent species $HMPH_2$, and that **3a–c** are the trivalent derivatives H_2MPH , where $M = Al$ (**1a–3a**), Ga (**1b–3b**), or In (**1c–3c**). The assignments will be justified by consideration of the frequencies and isotopic shifts of the observed bands and by reference to the vibrational properties of the molecules anticipated by DFT calculations; supporting evidence will also be sought from the vibrational properties established for related species.

$M\cdot PH_3$ (1a–c**).** In view of the reaction of Al, Ga, or In atoms with NH_3 ,⁹ similar behavior is likely to occur upon codeposition of the metal atoms with PH_3 . Indeed, the observed IR signatures of each of the products **1a–1c** are wholly consistent with the presence of a PH_3 molecule perturbed by such an interaction, and the dependence of their intensities on the PH_3 concentration supports the formulation $M\cdot PH_3$. The IR absorptions at 974.7, 973.6, and 974.4 cm^{-1} for **1a**, **1b**, and **1c**, respectively, can each be assigned to the symmetric PH_3 deformation mode of the relevant adduct $M\cdot PH_3$. Hence, it appears that the modes are *red*-shifted with respect to uncoordinated PH_3 (for which $\nu_2 = 993.8$ cm^{-1} ¹⁸). In the case of the ammonia adducts $M\cdot NH_3$, the symmetric NH_3 deformation mode is *blue*-shifted (by 156.9, 129.7, and 108.4 cm^{-1} for $M = Al, Ga, \text{ and } In$, respectively).⁹ Such a blue shift can be explained by metal-to-ligand charge transfer. The $M\cdots N$ interaction in $M\cdot NH_3$ appears therefore to be different from the $M\cdots P$ one in $M\cdot PH_3$. Recent theoretical studies of $Al\cdot PH_3$ suggest that the aluminum atom carries only a slight positive charge (+0.04 e).²⁵ This may also explain the finding that the ammonia adduct is clearly recognizable by its distinctive visible absorption band near 440 nm,⁹ whereas no similar band has been detected for the phosphine adduct. The characteristic electronic transition of the ammonia adduct can be associated with what is essentially a metal-based $^2S \leftarrow ^2P$ transition red-shifted under the action of charge transfer from the NH_3 .

DFT calculations find a global minimum for the ground state of an $M\cdot PH_3$ molecule with the geometry represented in Figure 5a; the optimized dimensions and vibrational properties are given in Table 4. Each of the molecules is found geometrically

Table 4. Comparison between the IR Spectra Observed and Calculated (Frequencies in cm^{-1}) for $M\cdot PH_3/M\cdot PD_3$ ($M = Al, Ga, \text{ or } In$)

$M\cdot PH_3$		$M\cdot PD_3$		assign	vibrational mode
obsd	calcd ^a	obsd	calcd ^a		
$M = Al$					
<i>b</i>	2411.9 (25)	<i>b</i>	1732.8 (14)	ν_1 (a')	$\nu_{\text{asym}}(P-H)$
2285.5	2334.7 (375)	1659.4	1670.7 (200)	ν_2 (a')	$\nu_{\text{sym}}(P-H)$
1101.2	1156.2 (101)	793.7	825.2 (53)	ν_3 (a')	$\delta_{\text{asym}}(PH_3)$
974.7	1025.1 (137)	718.3	750.4 (65)	ν_4 (a')	$\delta_{\text{sym}}(PH_3)$
<i>b</i>	238.4 (21)	<i>b</i>	181.2 (13)	ν_5 (a')	$\rho(PH_3)$
<i>c</i>	135.9 (1)	<i>c</i>	130.0 (0.4)	ν_6 (a')	$\nu(Al-P)$
<i>b</i>	2299.1 (62)	<i>b</i>	1654.9 (33)	ν_7 (a'')	$\nu_{\text{asym}}(P-H)$
<i>b</i>	1091.6 (10)	<i>b</i>	779.9 (5)	ν_8 (a'')	$\delta_{\text{asym}}(PH_3)$
<i>c</i>	195.3 (8)	<i>c</i>	145.1 (3)	ν_9 (a'')	$\rho(PH_3)$
$M = Ga$					
<i>b</i>	2408.3 (33)	<i>b</i>	1730.3 (19)	ν_1 (a')	$\nu_{\text{asym}}(P-H)$
2280.8	2346.8 (316)	1660.3	1679.6 (170)	ν_2 (a')	$\nu_{\text{sym}}(P-H)$
1108.2	1158.7 (86)	795.9	827.0 (45)	ν_3 (a')	$\delta_{\text{asym}}(PH_3)$
973.6	1025.7 (141)	717.7	750.5 (69)	ν_4 (a')	$\delta_{\text{sym}}(PH_3)$
<i>b</i>	210.2 (15)	<i>b</i>	159.5 (9)	ν_5 (a')	$\rho(PH_3)$
<i>c</i>	110.9 (0.1)	<i>c</i>	104.7 (0.02)	ν_6 (a')	$\nu(Ga-P)$
<i>b</i>	2318.6 (57)	<i>b</i>	1668.7 (30)	ν_7 (a'')	$\nu_{\text{asym}}(P-H)$
<i>b</i>	1107.2 (10)	<i>b</i>	790.9 (5)	ν_8 (a'')	$\delta_{\text{asym}}(PH_3)$
<i>c</i>	173.3 (8)	<i>c</i>	128.2 (4)	ν_9 (a'')	$\rho(PH_3)$
$M = In$					
<i>b</i>	2440.6 (36)	<i>b</i>	1754.2 (22)	ν_1	$\nu_{\text{asym}}(P-H)$
<i>b</i>	2412.3 (176)	<i>b</i>	1731.6 (32)	ν_2	$\nu_{\text{sym}}(P-H)$
<i>b</i>	2406.7 (61)	<i>b</i>	1726.2 (94)	ν_3	$\nu_{\text{asym}}(P-H)$
1105.7	1167.5 (40)	<i>b</i>	833.2 (20)	ν_4	$\delta_{\text{asym}}(PH_3)$
<i>b</i>	1142.4 (9)	<i>b</i>	815.5 (4)	ν_5	$\delta_{\text{asym}}(PH_3)$
974.4	1042.0 (146)	717.6	762.1 (73)	ν_6	$\delta_{\text{sym}}(PH_3)$
<i>c</i>	169.4 (14)	<i>c</i>	127.3 (8)	ν_7	$\rho(PH_3)$
<i>c</i>	151.4 (6)	<i>c</i>	111.1 (3)	ν_8	$\rho(PH_3)$
<i>c</i>	79.2 (0.4)	<i>c</i>	75.0 (0.2)	ν_9	$\nu(In-P)$

^a $Al\cdot PH_3$ symmetry C_s : $Al-P$ 2.7755 Å, $P-H(1,2)$ 1.4249 Å, $P-H(3)$ 1.4178 Å, $Al-P-H(1,2)$ 129.4°, $Al-P-H(3)$ 100.4°, $H(1)-P-H(2,3)$ 96.2°, $H(2)-P-H(3)$ 95.3°. $Ga\cdot PH_3$ symmetry C_s : $Ga-P$ 2.8411 Å, $P-H(1,2)$ 1.4238 Å, $P-H(3)$ 1.4185 Å, $Ga-P-H(1,2)$ 129.5°, $Ga-P-H(3)$ 101.1°, $H(1)-P-H(2,3)$ 95.8°, $H(2)-P-H(3)$ 95.0°. $In\cdot PH_3$ symmetry C_1 : $In-P$ 3.2219 Å, $P-H(1)$ 1.4228 Å, $P-H(2)$ 1.4209 Å, $P-H(3)$ 1.4227 Å, $In-P-H(1)$ 128.4°, $In-P-H(2)$ 106.2°, $In-P-H(3)$ 127.9°, $H(1)-P-H(2)$ 95.2°, $H(1)-P-H(3)$ 95.0°, $H(2)-P-H(3)$ 95.2°. Intensities ($km\ mol^{-1}$) are given in parentheses. ^b Too weak to be detected or hidden by phosphine absorptions. ^c Out of range of detection.

to resemble its ammonia counterpart⁹ in deviating slightly from regular C_{3v} symmetry; this is achieved through one $P-H$ bond being slightly shorter than the other two and the $H-P-H$ angles being fractionally different so that the overall symmetry is C_s and there are as a result not six but nine distinct vibrational fundamentals. At 2.7755, 2.8411, and 3.2219 Å, the calculated $M\cdots P$ distances in $Al\cdot PH_3$, $Ga\cdot PH_3$, and $In\cdot PH_3$, respectively, are shorter than the sums of the relevant van der Waals radii²⁶ by margins ranging from ca. 1.2 Å for Al to 0.6 Å for In. The estimated binding energies of 21.8, 22.1, and 17.0 $kJ\ mol^{-1}$ for $M = Al, Ga, \text{ and } In$, respectively, are significantly smaller than those for the corresponding ammonia complexes (60.2, 51.8, and 28.8 $kJ\ mol^{-1}$).⁹

Comparisons between the IR spectra observed and those predicted are severely limited by the weakness of many of the transitions in IR absorption and by the masking effects of bands due to free PH_3 or $[PH_3]_n$.¹⁸ Nevertheless, the features that could be observed for each complex were in satisfactory agreement with the properties forecast by the DFT calculations. We note particularly that the calculations anticipate not only that the

(25) Davy, R. D.; Schaefer, H. F., III. *J. Phys. Chem. A* **1997**, *101*, 3135.

(26) Nguyen, M. T.; McGinn, M. A.; Hegarty, A. F. *Inorg. Chem.* **1986**, *25*, 2185.

symmetric $\delta(\text{PH}_3)$ mode will give a relatively intense IR absorption but also that it will be *red*-shifted with respect to the corresponding mode of free PH_3 . The calculated shifts of 25.2, 24.6, and 8.3 cm^{-1} for $\text{M} = \text{Al}$, Ga , and In , respectively, may be compared with the experimental shifts of ca. 21, 22, and 23 cm^{-1} . Each of the bands observed at 2285.5 (**1a**) and 2280.8 cm^{-1} (**1b**) is readily attributed to the symmetric $\nu(\text{P-H})$ mode in the relevant complex on the evidence of the calculations and of the measured H/D shift. By the same criteria we are led to associate each of the weak bands at 1101.2, 1108.2, and 1105.7 cm^{-1} with the antisymmetric $\delta(\text{PH}_3)$ (a') fundamental.

The $\nu_{\text{sym}}(\text{P-H})$ and $\delta_{\text{sym}}(\text{PH}_3)$ frequencies determined here are comparable with those displayed by PH_3 in transition metal complexes. Thus, $\nu(\text{P-H})$ modes with frequencies of 2250, 2270, and 2383/2393 cm^{-1} have been identified for $\text{Cu}(\text{PH}_3)_n$ ($n = 1-3$),⁶ $\text{Ni}(\text{PH}_3)_4$,^{6,7} and $\text{H}_3\text{P}\cdot\text{TiCl}_4$,⁸ respectively; $\delta_{\text{sym}}(\text{PH}_3)$ for the same species is reported to occur at 958–970, 998, and 967 cm^{-1} .

The absorptions at 971.2, 969.3, and 968.0 cm^{-1} for Al , Ga , and In , respectively, can be assigned to the 1:2 complexes $\text{M}(\text{PH}_3)_2$ on the basis of the experiments with different PH_3 concentrations. Calculations have been performed in the search for information about the likely structure of such a species. The optimized geometries exhibit C_{2v} symmetry (Figure 5b) and P-M-P angles of 83.2, 85.5, and 79.4° for $\text{M} = \text{Al}$, Ga , and In , respectively. Hence, the angles are comparable with those calculated for complexes of the types $\text{M}(\text{N}_2)_2$ (75.3°, 79.3°, and 67.1°)²⁷ and $\text{M}(\text{CO})_2$ (73.5°, 72.6°, and 61.8°).²⁸ The $\text{M}\cdots\text{P}$ distances in the 1:2 complexes are estimated to be 2.7013, 2.8011, and 3.1457 Å, i.e., somewhat shorter than those in the 1:1 complexes (2.7755, 2.8411, and 3.2219 Å).

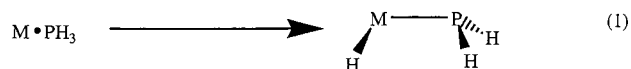
The $\delta_{\text{sym}}(\text{PH}_3)$ modes of $\text{M}(\text{PH}_3)_2$ ($\text{M} = \text{Al}$, Ga , and In) are calculated to occur at 1026.9 (253), 1023.6 (242), and 1039.0 (194) cm^{-1} , respectively (the intensities in km mol^{-1} being given in parentheses). Thus, they are shifted by +1.8, –2.1, and –3.0 cm^{-1} from the corresponding frequencies of the $\text{M}\cdot\text{PH}_3$ adducts. These values compare with the observed shifts of –3.5, –4.3, and –6.4 cm^{-1} , which show the same trend in the series $\text{M} = \text{Al}$, Ga , and In .

The calculated binding energies of the $\text{M}\cdot\text{PH}_3$ and $\text{M}(\text{PH}_3)_2$ complexes may be compared with the values obtained for other complexes. For example, the 1:1 complexes of Al with N_2 ,²⁷ PH_3 , NH_3 ,⁹ and CO ²⁸ exhibit binding energies of –16.4, –21.8, –60.2, and –81 kJ mol^{-1} , respectively. Thus, the ligand–metal interaction increases in the order $\text{N}_2 < \text{PH}_3 < \text{NH}_3 < \text{CO}$. The same trend is observed for the 1:1 complexes of Ga (energies in kJ mol^{-1} , $\text{Ga}\cdot\text{N}_2$ –8.4, $\text{Ga}\cdot\text{PH}_3$ –22.1, $\text{Ga}\cdot\text{NH}_3$ –51.8, $\text{Ga}\cdot\text{CO}$ –61) and In (energies in kJ mol^{-1} , $\text{In}\cdot\text{N}_2$ 7.0, $\text{In}\cdot\text{PH}_3$ –17.0, $\text{In}\cdot\text{NH}_3$ –28.8, $\text{In}\cdot\text{CO}$ –43). The 1:2 complexes $\text{M}(\text{N}_2)_2$, $\text{M}(\text{CO})_2$, and $\text{M}(\text{PH}_3)_2$ each have a total binding energy slightly greater than twice the value associated with the corresponding 1:1 complex, the only exception being $\text{Al}(\text{N}_2)_2$ [energies in kJ mol^{-1} , $\text{Al}(\text{N}_2)_2$ –26.4, $\text{Al}(\text{CO})_2$ –176, $\text{Al}(\text{PH}_3)_2$ –48.9, $\text{Ga}(\text{N}_2)_2$ –17.1, $\text{Ga}(\text{CO})_2$ –125, $\text{Ga}(\text{PH}_3)_2$ –45.0, $\text{In}(\text{N}_2)_2$ –14.6, $\text{In}(\text{CO})_2$ –85, $\text{In}(\text{PH}_3)_2$ –34.1]. A remarkable aspect of these results is the relatively strong binding of CO by the main group metals Al , Ga , and In .

HMPH₂ (2a–c). As noted previously, the IR bands of **2a**–**2c** at 1768.2, 1721.4, and 1546.4 cm^{-1} are each highly suggestive of a $\nu(\text{M-H})$ fundamental of a *divalent* group 13

metal hydride, a view supported by the H/D isotopic shifts displayed by the relevant features of **2a** and **2b**. Analogy with the corresponding reactions of the metal atoms with ammonia⁹ gives further persuasive backing to the belief that photolysis of the adduct $\text{M}\cdot\text{PH}_3$ at wavelengths near 436 nm yields the insertion product HMPH_2 , where $\text{M} = \text{Al}$ (**2a**), Ga (**2b**), or In (**2c**). Furthermore, the UV–vis spectrum of the photolyzed matrix containing **2a** and the photochemical behaviors of all three products indicate that each has an electronic transition near 550 nm, excitation into which results in photodissociation of the molecule. This behavior is reminiscent of that reported by Lafleur and Parnis¹² for the matrix-isolated molecule $\text{CH}_3\text{-GaH}$, which was described as displaying a broad absorption near 600 nm, excitation into which led also to photodissociation of the molecule (although subsequent studies have revealed rather different properties¹³).

DFT calculations find an equilibrium geometry with only C_1 symmetry for each of the molecules HMPH_2 , as illustrated in Figure 5c, and with the dimensions given in Table 5. The lack of any symmetry reflects the tightly pyramidal disposition of the bonds about the P atom. By contrast, the analogous amides feature *planar* geometries at nitrogen, at least in the cases where $\text{M} = \text{Al}$ or Ga . The M-P bonds measure 2.3713 ($\text{M} = \text{Al}$), 2.3919 ($\text{M} = \text{Ga}$), and 2.6031 Å ($\text{M} = \text{In}$), i.e., 0.55–0.61 Å longer than the M-N bonds in the corresponding amides;⁹ the normally accepted covalent radii of N and P ²⁶ differ by only 0.36 Å. In addition, the reaction energies for the transformation (eq 1) are calculated to be –72.7, –22.3, and +6.6 kJ mol^{-1}



for $\text{M} = \text{Al}$, Ga , and In , respectively; these are similar to, or up to 30 kJ mol^{-1} more exoergic than, the energies estimated at the same level of theory for the corresponding rearrangement of $\text{M}\cdot\text{NH}_3$.⁹

Out of the nine IR-active vibrational fundamentals expected for each of the HMPH_2 molecules, no more than four, three, and two have been observed for $\text{M} = \text{Al}$, Ga , and In , respectively, in one isotopic version or another. The calculations indicate that the $\nu(\text{P-H})$ absorptions of the products are liable to be obscured by those due to free PH_3 . Otherwise, it has been possible to locate most of the transitions expected to have appreciable intensity in IR absorption, and the observed frequencies and relative intensities are invariably consistent with the calculated properties (see Table 5). The $\nu(\text{M-H})$ fundamental is predicted to give what is by some margin the most intense IR absorption, and this has been observed in all three cases. Significantly weaker bands in the spectra of **2a** and **2b** can be satisfactorily attributed to the PH_2 scissoring mode [at 1159.4 (**2a**) and 1060.9 cm^{-1} (**2b**)] and M-H in-plane deformation [at 403.9 (**2a**) and 428.2 cm^{-1} (**2b**)], while a band at 727.1 cm^{-1} in the spectrum of **2a** also finds a ready explanation in the PH_2 wagging mode.

H₂MPH (3a–c). The IR absorptions of **3a** at 1874.1/1866.1 and 765.9 cm^{-1} and those of **3b** at 1897.5/1893.3 and 738.9 cm^{-1} are typical of the stretching and scissoring vibrations of MH_2 groups in trivalent derivatives of aluminum and gallium. It is likely that the corresponding high-frequency feature of **3c** (expected near 1700 cm^{-1}) is obscured by absorptions due to traces of water impurity, but a weak band due to **3c** at 674.7 cm^{-1} is a plausible candidate for a $\delta(\text{InH}_2)$ mode.^{9,15a}

At this stage, there are notable differences between the results of the phosphine experiments and those of the ammonia

(27) Himmel, H.-J.; Downs, A. J.; Greene, T. M. Unpublished results.

(28) Himmel, H.-J.; Downs, A. J.; Green, J. C.; Greene, T. M. *J. Phys. Chem. A* **2000**, *104*, 3642.

Table 5. Comparison between the IR Spectra Observed and Calculated (Frequencies in cm^{-1}) for $\text{HMPH}_2/\text{DMPD}_2$ ($M = \text{Al, Ga, or In}$)

HMPH ₂		DMPD ₂		assignt	vibrational mode
obsd	calcd ^a	obsd	calcd ^a		
M = Al					
<i>b</i>	2375.2 (54)	<i>b</i>	1706.6 (27)	ν_1	$\nu_{\text{sym}}(\text{P-H})$
<i>b</i>	2341.8 (52)	<i>b</i>	1680.2 (26)	ν_2	$\nu_{\text{asym}}(\text{P-H})$
1768.2	1826.7 (260)	1288.4	1315.5 (139)	ν_3	$\nu(\text{Al-H})$
1159.4	1120.8 (19)	<i>b</i>	805.4 (8)	ν_4	PH_2 scissoring
727.1	691.0 (33)	532.3	509.3 (25)	ν_5	PH_2 wagging
<i>b</i>	452.9 (22)	<i>b</i>	380.9 (22)	ν_6	PH_2 out-of-plane rock
403.9	426.3 (55)	<i>b</i>	330.8 (8)	ν_7	Al-H in-plane deformation
<i>b</i>	372.8 (12)	<i>b</i>	294.3 (20)	ν_8	$\nu(\text{Al-P})$
<i>b</i>	235.3 (6)	<i>c</i>	170.3 (3)	ν_9	Al-H out-of-plane deformation
M = Ga					
<i>b</i>	2369.8 (55)	<i>b</i>	1702.8 (28)	ν_1	$\nu_{\text{sym}}(\text{P-H})$
<i>b</i>	2337.8 (52)	<i>b</i>	1677.5 (27)	ν_2	$\nu_{\text{asym}}(\text{P-H})$
1721.4	1740.6 (303)	1244.7	1240.3 (156)	ν_3	$\nu(\text{Ga-H})$
1060.9	1122.0 (19)	<i>b</i>	805.8 (9)	ν_4	PH_2 scissoring
<i>b</i>	683.9 (10)	<i>b</i>	495.8 (7)	ν_5	PH_2 wagging
<i>b</i>	463.0 (12)	<i>b</i>	342.9 (7)	ν_6	PH_2 out-of-plane rock
428.2	412.9 (33)	<i>b</i>	297.3 (19)	ν_7	Ga-H in-plane deformation
<i>b</i>	292.6 (11)	<i>b</i>	279.6 (7)	ν_8	$\nu(\text{Ga-P})$
<i>b</i>	227.2 (3)	<i>c</i>	163.4 (2)	ν_9	Ga-H out-of-plane deformation
M = In					
<i>b</i>	2408.2 (54)	<i>b</i>	1730.3 (27)	ν_1	$\nu_{\text{sym}}(\text{P-H})$
2299.4	2373.3 (55)	<i>b</i>	1703.0 (28)	ν_2	$\nu_{\text{asym}}(\text{P-H})$
1546.4	1570.4 (320)	1114.9	1115.8 (163)	ν_3	$\nu(\text{In-H})$
<i>b</i>	1136.7 (17)	<i>b</i>	816.4 (8)	ν_4	PH_2 scissoring
<i>b</i>	643.1 (23)	<i>b</i>	463.5 (14)	ν_5	PH_2 wagging
<i>b</i>	474.2 (7)	<i>b</i>	347.6 (5)	ν_6	PH_2 out-of-plane rock
<i>b</i>	374.5 (41)	<i>b</i>	266.9 (21)	ν_7	In-H in-plane deformation
<i>b</i>	244.0 (8)	<i>b</i>	236.9 (6)	ν_8	$\nu(\text{In-P})$
<i>c</i>	175.9 (4)	<i>c</i>	125.9 (2)	ν_9	In-H out-of-plane deformation

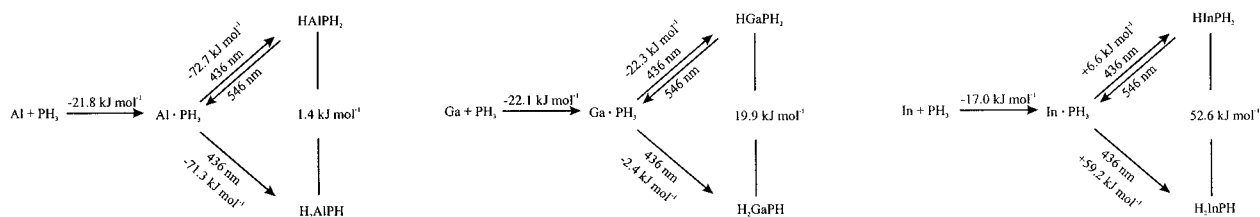
^a HAIPH₂ symmetry C_1 : Al-H 1.6065 Å, Al-P 2.3713 Å, P-H 1.4222/1.4268 Å, H-Al-P 114.4°, Al-P-H 97.8/94.6°, H-P-H 94.9°. HGaPH₂ symmetry C_1 : Ga-H 1.6117 Å, Ga-P 2.3919 Å, P-H 1.4227/1.4278 Å, H-Ga-P 115.4°, Ga-P-H 96.8/92.3°, H-P-H 94.3°. HInPH₂ symmetry C_1 : In-H 1.7762 Å, In-P 2.6031 Å, P-H 1.4245/1.4296 Å, H-In-P 115.3°, In-P-H 95.7/93.0°, H-P-H 93.8°. Intensities (km mol^{-1}) are given in parentheses. ^b Too weak to be detected or hidden by phosphine absorptions. ^c Out of range of detection.

experiments.⁹ There are several reasons for concluding that the trivalent species **3a-c** are *not* the derivatives H_2MPH_2 , suggested by analogy with the ammonia reactions, but the radicals H_2MPH . Ammonia-doped matrices yielded *only* HMNH_2 following photolysis at $\lambda = 436$ nm. The trivalent derivative H_2MNH_2 ($M = \text{Al, Ga, or In}$) was formed only when the matrix was subsequently irradiated with broad-band UV-visible light ($200 \leq \lambda \leq 800$ nm). This was a photostable end-product of the reactions, together with the univalent derivative MNH_2 .⁹ By contrast, the trivalent species **3a-c** identified in the phosphine experiments made their first appearance *at the outset* of photolysis at $\lambda = 436$ nm and all the detectable products containing metal and phosphorus, including **3a-c**, were observed to be destroyed by photolysis with broad-band UV-visible light. Furthermore, the insertion product HMNH_2 can be shown unequivocally to be the precursor to the trivalent product H_2MNH_2 . Yet the compounds **3a-c** are formed independently of HMPH_2 on photolysis of $\text{M}\cdot\text{PH}_3$ at $\lambda = 436$ nm; selective destruction of HMPH_2 by irradiation at $\lambda = 546$ nm did not lead to a corresponding buildup of the product **3**. The decomposition of HMPH_2 can proceed through several channels, including the regeneration of the adduct $\text{M}\cdot\text{PH}_3$ and the formation of PH , presumably together with M atoms and H_2 (see below). An essential part of the clearly implied mechanism affording the photostable end-products of the M/NH_3 reactions involves the abstraction of H atoms from HMNH_2 to give the photostable M(I) amide MNH_2 . In the experiments with PH_3 , however, there was no spectroscopic hint of MPH_2 . Moreover, the IR spectra attested to the formation of significant amounts of **3a-c** even after very brief periods of photolysis

(<1 min at $\lambda = 436$ nm). The buildup of H_2MNH_2 was, by contrast, a delayed process, requiring long photolysis times (30 min and more at $200 \leq \lambda \leq 800$ nm). With very low concentrations of NH_3 , only HMNH_2 and MNH_2 were detected in appreciable concentrations, to the virtual exclusion of H_2MNH_2 .⁹ In the experiments with PH_3 , low concentrations of PH_3 caused a decrease in the intensities of all the product bands, but the relative intensities of these bands underwent little change.

Theoretical (DFT) investigations show that the H_2MPH radical has a ground-state energy very close to that of HMPH_2 . Hence, H_2MPH , featuring a trivalent metal center and a divalent phosphorus one, emerges as a relatively stable molecule likely to be formed in the course of the photoinduced reactions occurring between Al, Ga, or In atoms and PH_3 .²⁵ It thus differs from H_2MNH , a high-energy species that is not expected to be generated under these conditions.²⁶ The energy difference between H_2MPH and HMPH_2 is estimated to be +1.4, +19.9, and +52.6 kJ mol^{-1} for $M = \text{Al, Ga, and In}$, respectively (see Scheme 1). In the calculations at the TZ2P CCSD level performed by Davy and Schaefer,²⁵ H_2AlPH comes out to be even slightly lower in energy than HAIPH_2 . The experimental proportions of the two products **2a-c** and **3a-c** reflect appealingly the trend toward higher energy of the H_2MPH isomer relative to HMPH_2 , the proportion **3/2** decreasing in the order $\text{Al} > \text{Ga} > \text{In}$.

For all these reasons the compounds **3a-c** were identified as H_2AlPH , H_2GaPH , and H_2InPH , respectively. According to DFT calculations, again by use of the B3LYP hybrid method,¹⁷ of the possible configurations open to a molecule of the form H_2MPH , that with the structure depicted in Figure 5d is lowest

Scheme 1. Pathways and Relative Energies for the Reactions of Al, Ga, and In with PH₃, Leading to M·PH₃, HMPH₂, and H₂MPH**Table 6.** Comparison between the IR Spectra Observed and Calculated (Frequencies in cm⁻¹) for H₂MPH/D₂MPD (M = Al, Ga, or In)

H ₂ MPH		D ₂ MPD		assign	vibrational mode
obsd	calcd ^a	obsd	calcd ^a		
M = Al					
<i>b</i>	2312.9 (78)	<i>b</i>	1661.1 (39)	ν_1	$\nu(\text{P-H})$
1874.7	1953.2 (244)	1373.5	1416.7 (140)	ν_2	$\nu_{\text{asym}}(\text{Al-H})$
1866.1	1936.9 (168)	1345.6	1382.5 (96)	ν_3	$\nu_{\text{sym}}(\text{Al-H})$
765.9	781.8 (349)	564.5	574.0 (196)	ν_4	AlH ₂ bend
606.3	670.0 (36)	482.8	500.3 (27)	ν_5	H-P-Al bend
569.0	518.9 (179)	<i>b</i>	385.6 (96)	ν_6	AlH ₂ wag
<i>b</i>	408.6 (13)	<i>b</i>	393.3 (8)	ν_7	$\nu(\text{Al-P})$
<i>b</i>	393.1 (49)	<i>b</i>	285.4 (27)	ν_8	AlH ₂ rock
<i>c</i>	85.0 (8)	<i>c</i>	60.9 (5)	ν_9	H-P-Al-H torsion
M = Ga					
<i>b</i>	2308.2 (74)	<i>b</i>	1657.8 (37)	ν_1	$\nu(\text{P-H})$
1897.5	1960.4 (239)	1372.8	1400.2 (129)	ν_2	$\nu_{\text{asym}}(\text{Ga-H})$
1893.3	1948.2 (167)	1360.1	1382.9 (84)	ν_3	$\nu_{\text{sym}}(\text{Ga-H})$
738.9	735.4 (229)	528.8	524.6 (119)	ν_4	GaH ₂ bend
646.5/644.8	673.7 (23)	486.4	495.0 (12)	ν_5	H-P-Ga bend
454.8	501.0 (84)	<i>b</i>	362.6 (45)	ν_6	GaH ₂ wag
<i>b</i>	373.0 (34)	<i>b</i>	268.7 (17)	ν_7	GaH ₂ rock
<i>b</i>	335.2 (11)	<i>b</i>	331.0 (11)	ν_8	$\nu(\text{Ga-P})$
<i>c</i>	107.9 (5)	<i>c</i>	77.4 (3)	ν_9	H-P-Ga-H torsion
M = In					
<i>b</i>	2355.9 (76)	<i>b</i>	1692.1 (37)	ν_1	$\nu(\text{P-H})$
<i>b</i>	1735.6 (194)	<i>b</i>	1232.2 (120)	ν_2	$\nu_{\text{asym}}(\text{In-H})$
<i>b</i>	1723.6 (252)	<i>b</i>	1224.4 (110)	ν_3	$\nu_{\text{sym}}(\text{In-H})$
<i>b</i>	656.3 (39)	<i>b</i>	476.8 (9)	ν_4	InH ₂ bend
674.7	634.8 (304)	<i>b</i>	452.8 (167)	ν_5	H-P-In bend
<i>b</i>	456.5 (141)	<i>b</i>	328.2 (74)	ν_6	InH ₂ wag
<i>b</i>	329.2 (40)	<i>b</i>	236.4 (20)	ν_7	InH ₂ rock
<i>b</i>	280.3 (10)	<i>b</i>	276.8 (11)	ν_8	$\nu(\text{In-P})$
<i>c</i>	80.0 (7)	<i>c</i>	57.4 (4)	ν_9	H-P-In-H torsion

^a H₂AlPH symmetry C₁: Al-H 1.5854/1.5836 Å, Al-P 2.3523 Å, P-H 1.4319 Å, H-Al-H 120.9°, H-Al-P 118.4°, Al-P-H 93.0°, H-Al-P-H 154.8°. H₂GaPH symmetry C₁: Ga-H 1.5732/1.5717 Å, Ga-P 2.3421 Å, P-H 1.4324 Å, H-Ga-H 120.8°, H-Ga-P 119.6/119.5°, Ga-P-H 92.1°. H₂InPH symmetry C₁: In-H 1.7349/1.7326 Å, In-P 2.5554 Å, P-H 1.4335 Å, H-In-H 121.5°, H-In-P 120.2/118.3°, In-P-H 92.7°. Intensities (km mol⁻¹) are given in parentheses.

^b Too weak to be detected or hidden by phosphine absorptions. ^c Out of range of detection.

in energy. Details of the calculated dimensions, together with the vibrational frequencies and IR intensities, are given in Table 6. Hence, it is apparent that the calculated vibrational properties are in good agreement with the experimental findings for **3a**–**3c**. The structure thus calculated for H₂AlPH is also in good agreement with the results of earlier theoretical studies.²⁵

With overall symmetry no higher than C₁, the H₂MPH molecule is expected to have nine vibrational fundamentals. Five of these, predicted to be among the most intense in IR absorption, have been satisfactorily and severally identified for **3a** and **3b**, and the fundamental predicted to be most intense at frequencies less than 1500 cm⁻¹ has likewise been identified

for **3c**. There can be little doubt about the assignment of the symmetric and antisymmetric $\nu(\text{M-H})$ modes of **3a** and **3b**. Moreover, the frequencies and relative intensities of the absorptions observed at 765.9, 738.9, and 674.7 cm⁻¹ for **3a**, **3b**, and **3c**, respectively, give every reason to believe that they originate in the appropriate MH₂ scissoring mode. The M-P-H bending vibration ν_6 is presumably the author of the bands at 606.3 (**3a**) and 646.5/644.8 cm⁻¹ (**3b**). The bands that have not so far been accounted for, at 569.0 and 454.8 cm⁻¹ in the spectra of **3a** and **3b**, can then be plausibly associated with the appropriate MH₂ wagging fundamental. This mode is actually calculated to be more intense in IR absorption than the M-P-H bending mode. However, the relative intensities of these two bands were found to vary widely as the PH unit was caused to rotate relative to the MH₂ unit, a motion opposed by a very low barrier (<1 kJ mol⁻¹). Where H/D shifts could be measured, they are wholly supportive of the present assignments.

An unusual feature in the IR spectra of H₂AlPH and H₂GaPH is the increase of the energy difference between the $\nu_{\text{asym}}(\text{MH}_2)$ and the $\nu_{\text{sym}}(\text{MH}_2)$ fundamentals when hydrogen is replaced by deuterium, amounting to 19.3 and 8.5 cm⁻¹ for M = Al and Ga, respectively (see Figures 1b and 2b). The calculated IR frequencies show the same behavior (with increases of 16.9 and 5.1 cm⁻¹ for Al and Ga, respectively). Coupling of the $\nu(\text{M-H})$ fundamentals with modes of the MPH group is responsible for this behavior. The coupling has consequences too for the intensities of the relevant absorptions. For an H-M-H bond angle near 121° a ratio $I_{\text{asym}}/I_{\text{sym}}$ near 3.2:1 is expected in the absence of coupling. The intensities observed^{15a} for H₂InCl are indeed in good agreement with this estimate. However, the observed and calculated ratios for H₂MPH are much smaller and, in the absence of any coupling effects, seem to imply a significantly smaller H-M-H angle. For GaH₂, the calculations predict that $I_{\text{asym}}/I_{\text{sym}} = 4.38:1$ [with the frequencies being located at 1833.2 (*b*₂) and 1760.0 (*a*₁) cm⁻¹] and a bond angle of 119.5°. At the same level of theory, the calculations predict ratios and angles of 4.55:1 and 131.9°, 3.56:1 and 124.4°, 3.83:1 and 126.7°, 1.45:1 and 120.9°, and 1.43:1 and 120.8° for H₂InCl, H₂AlNH₂, H₂GaNH₂, H₂AlPH, and H₂GaPH, respectively. These figures demonstrate some of the dangers of trying to estimate the H-M-H bond angle from the ratio $I_{\text{asym}}/I_{\text{sym}}$.²⁷

The doublet features at 1867.4/1860.6 and 1918.4/1913.2 cm⁻¹ in the experiments with Al and Ga, respectively, are most likely to be associated with the phosphine adducts H₂AlPH·PH₃ and H₂GaPH·PH₃. At low PH₃ concentrations, these signals were seen to be much reduced in intensity relative to the signals due to other species.

PH_n (*n* = 1, 2, 4, or 5). The features of the IR spectra that have yet to be explained are the absorption at 2248.9 cm⁻¹ appearing after photolysis of matrices containing either Ga or In and PH₃ and its counterpart at 1641.3 cm⁻¹ in the experiments with PD₃ (H/D = 1.3708). Because of the frequency invariance of this signal irrespective of the metal, it is unlikely to originate

in a metal derivative. The large H/D shift shows, on the other hand, that the absorber contains one or more hydrogen atoms. P_2H_4 can be excluded because the spectra show no evidence for any other signals, e.g., near 800 cm^{-1} where the PH_2 twisting mode is expected to occur with significant intensity.³¹ The species is thus most likely to be a molecule of the type PH_n . The measured (anharmonic) vibrational frequency of gaseous PH is 2276 cm^{-1} ,³² whereas $\delta(\text{PH}_2)$, which carries most of the intensity in IR absorption, has been reported to occur at 1103 cm^{-1} for PH_2 isolated in an Ar matrix.³³ Our calculations give the following vibrational frequencies (in cm^{-1}) for the molecules PH, PH_2 (C_{2v}), PH_4 (C_{2v}), and PH_5 (D_{3h}), the IR intensities (in km mol^{-1}) being given in parentheses: PH 2318.6 (109); PH_2 2337.4 (93) ν_1 (a_1), 1152.4 (32) ν_2 (a_1), 2344.2 (110) ν_3 (b_2); PH_4 (C_{2v}) 2435.5 (24) ν_1 (a_1), 1735.9 (6) ν_2 (a_1), 1015.1 (1) ν_3 (a_1), 896.1 (13) ν_4 (a_1), 1204.3 (0) ν_5 (a_2), 2447.7 (50) ν_6 (b_1), 810.0 (13) ν_7 (b_1), 1330.3 (446) ν_8 (b_2), 1123.8 (256) ν_9 (b_2); PH_5 (D_{3h}) 2282.5 (0) ν_1 (a_1'), 1843.9 (0) ν_2 (a_1'), 1926.0 (1112) ν_3 (a_2''), 1227.2 (338) ν_4 (a_2''), 2279.1 ν_5 (272) (e'), 1271.2 (436) ν_6 (e'), 498.2 (20) ν_7 (e'), 1483.6 (0) ν_8 (e''). The $\nu(\text{P-H})$ fundamentals of PH_3 are calculated to occur at 2370.8 (54) ν_1 (a_1) and 2377.1 cm^{-1} (186) ν_3 (e). The frequency observed for the unknown PH_n species is shifted by about -93 cm^{-1} with respect to the $\nu(\text{P-H})$ frequencies of matrix-isolated PH_3 .¹⁸ On the basis of the previously published experimental results³³ and of our calculations, we can exclude PH_2 because there was no sign of a band near 1103 cm^{-1} , which should be the strongest feature; moreover, the predicted shift of about -30 cm^{-1} between the P-H stretching frequencies of PH_3 and PH_2 is too small. PH_4 can also be excluded because our calculations impute frequencies to two of the $\nu(\text{P-H})$ modes of this molecule that are *higher* than those of PH_3 . PH_5 is also unlikely to be responsible for the observed signals because there is no evidence of a feature near 1930 or 1270 cm^{-1} that tracks the one observed at 2248.9 cm^{-1} . Thus, the most likely author of the absorption at 2248.9 cm^{-1} in the experiments with PH_3 or its analogue at 1641.3 cm^{-1} in the experiments with PD_3 is PH or PD. The frequencies of the gaseous molecules PH and PD (2276 and 1653 cm^{-1} , respectively), giving an H/D ratio of 1.3768:1, are close to our values for Ar matrices, and the predicted shift of ca. -56 cm^{-1} with respect to the PH_3 stretching fundamentals is not too far out of line with the observed shift of ca. -93 cm^{-1} .

The signal that may be due to PH did not appear when the matrices contained only PH_3 in the absence of any metal atoms. This implies that the carrier is formed following the decomposition of the insertion product HMPH_2 , where $\text{M} = \text{Ga}$ or In .

H_2MPH_2 , MPH_2 , HMPH , and MP . Although we have no experimental evidence that any of these compounds is formed by the group 13 metals, the structures, IR spectra, and energies have been calculated because they are all potential products of photolytic reactions originating in HMPH_2 .

The vibrational frequencies and IR intensities, as well as the dimensions, of the H_2MPH_2 species ($\text{M} = \text{Al}$, Ga , or In) are given in Table 7. All three compounds are nonplanar (conform-

Table 7. Calculated IR Spectra (Frequencies in cm^{-1}) for H_2MPH_2 ($\text{M} = \text{Al}$, Ga , or In)^a

H_2AlPH_2	H_2GaPH_2	H_2InPH_2	assign	vibrational mode
2367.0 (50)	2367.3 (49)	2393.8 (49)	ν_1 (a')	$\nu_{\text{sym}}(\text{P-H})$
1942.9 (160)	1959.4 (158)	1736.4 (165)	ν_2 (a')	$\nu_{\text{sym}}(\text{M-H})$
1120.7 (30)	1125.2 (32)	1137.3 (27)	ν_3 (a')	$\delta(\text{PH}_2)$
778.1 (360)	741.8 (234)	640.1 (312)	ν_4 (a')	$\delta(\text{MH}_2)$
622.8 (119)	633.4 (51)	589.1 (81)	ν_5 (a')	twist
432.6 (53)	453.7 (45)	426.1 (87)	ν_6 (a')	$\rho_{\text{out-of-plane}}(\text{MH}_2)$
408.0 (24)	339.7 (16)	283.1 (12)	ν_7 (a')	$\nu(\text{M-P})$
2378.5 (57)	2379.0 (58)	2406.1 (61)	ν_8 (a'')	$\nu_{\text{asym}}(\text{P-H})$
1957.2 (244)	1972.5 (241)	1732.0 (277)	ν_9 (a'')	$\nu_{\text{asym}}(\text{M-H})$
682.6 (4)	690.1 (2)	661.3 (6)	ν_{10} (a'')	$\delta_{\text{in-plane}}(\text{PH}_2)$
370.4 (52)	369.4 (34)	316.5 (39)	ν_{11} (a'')	$\delta_{\text{in-plane}}(\text{MH}_2)$
214.6 (4)	226.1 (5)	184.6 (4)	ν_{12} (a'')	$\rho_{\text{out-of-plane}}(\text{PH}_2)$

^a H_2AlPH_2 symmetry C_s : Al-H 1.5837 Å, Al-P 2.3379 Å, P-H 1.4228 Å, H-Al-H 121.4°, H-Al-P 119.1°, H-P-H 95.7°, Al-P-H 96.9°, H-Al-P-H 141.6°. H_2GaPH_2 symmetry C_s : Ga-H 1.5704 Å, Ga-P 2.3310 Å, P-H 1.4227 Å, H-Ga-H 121.5°, H-Ga-P 119.1°, H-P-H 95.5°, Ga-P-H 96.3°. H_2InPH_2 symmetry C_s : In-H 1.7328 Å, In-P 2.5355 Å, P-H 1.4256 Å, H-In-H 121.7°, H-In-P 119.0°, H-P-H 94.6°, In-P-H 95.3°. Intensities (km mol^{-1}) are given in parentheses.

ing to C_s symmetry). On the evidence of these results, it is clear that the observed IR spectra of products **3a-c** could also be interpreted as arising from molecules of this type. As discussed above, however, the circumstances giving rise to **3a-c**, the behavior on photolysis, comparisons with the corresponding ammonia experiments,⁹ and the results of theoretical studies all lead to the conclusion that this product is not H_2MPH_2 but H_2MPH .

The equilibrium structures of MPH_2 (C_s), H_2MPH_2 , and HMPH (C_s) are illustrated in parts e, f, and g of Figure 5, respectively. As expected, the MPH_2 molecule is nonplanar, the M-P-H/H-P-H bond angles being $92.3/93.9^\circ$ ($\text{M} = \text{Al}$), $89.4/93.3^\circ$ ($\text{M} = \text{Ga}$), and $91.9/93.2^\circ$ ($\text{M} = \text{In}$). The corresponding M-P-P-H distances are 2.4490/1.4300, 2.4829/1.4320, and 2.6962/1.4317 Å. The six fundamentals spanning the irreducible representation $4a' + 2a''$ occur with the following frequencies (in cm^{-1}) and with the IR intensities (in km mol^{-1}) given in parentheses: AlPH_2 2312.8 (56) ν_1 (a'), 1104.1 (12) ν_2 (a'), 378.3 (75) ν_3 (a'), 320.8 (34) ν_4 (a'), 2322.9 (68) ν_5 (a''), 416.1 (70) ν_6 (a''); GaPH_2 2299.0 (65) ν_1 (a'), 1106.0 (17) ν_2 (a'), 381.2 (41) ν_3 (a'), 262.8 (37) ν_4 (a'), 2307.9 (80) ν_5 (a''), 427.2 (43) ν_6 (a''); and InPH_2 2349.9 (65) ν_1 (a'), 1122.2 (14) ν_2 (a'), 395.2 (32) ν_3 (a'), 226.6 (27) ν_4 (a'), 2359.9 (81) ν_5 (a''), 434.1 (36) ν_6 (a''). Perhaps the most noteworthy feature here is the weakness in IR absorption of all the transitions at frequencies less than 2000 cm^{-1} . Allied to the danger that the $\nu(\text{P-H})$ absorptions are obscured by the corresponding features of free PH_3 , this is likely to impair the detection of MPH_2 molecules at low concentration.

The HMPH molecules are, like their HMNH analogues,⁹ high-energy species, the energy for isomerization of MPH_2 to HMPH being $+43.5$, $+69.6$, and $+183.1\text{ kJ mol}^{-1}$ for $\text{M} = \text{Al}$, Ga , and In , respectively; the H-M-P/M-P-H angles are $177.1/84.3^\circ$, $177.3/85.9^\circ$, and $114.7/94.8^\circ$. The H-M/M-P-P-H bond lengths (in Å) are as follows: HAlPH 1.5794/2.1535/1.4431, HGAPH 1.5586/2.1445/1.4401, and HInPH 1.7792/2.6294/1.4308. Six vibrational modes exist, all of them IR-active, the frequencies (in cm^{-1}) and IR intensities (in km mol^{-1}) in parentheses being as follows: HAlPH 2238.4 (74) ν_1 (a'), 1960.0 (201) ν_2 (a'), 620.2 (14) ν_3 (a'), 522.1 (21) ν_4 (a'), 269.1 (43) ν_5 (a'), 352.2 (7) ν_6 (a''); HGAPH 2256.5 (59) ν_1 (a'), 1986.4 (199) ν_2 (a'), 678.1 (6) ν_3 (a'), 451.7 (10) ν_4 (a'), 349.9 (21) ν_5 (a'), 379.4 (0.1) ν_6 (a''); and HInPH 2373.0 (67) ν_1 (a'), 1564.1

(29) Davy, R. D.; Jaffrey, K. L. *J. Phys. Chem.* **1994**, *98*, 8930.

(30) Smit, W. M. A. *J. Mol. Struct.* **1973**, *19*, 789. Beattie, I. R.; Ogden, J. S.; Price, D. D. *J. Chem. Soc., Dalton Trans.* **1982**, 505.

(31) Rak, J.; Skurski, P.; Liwo, A.; Błażejowski, J. *J. Am. Chem. Soc.* **1995**, *117*, 2638. Durig, J. R.; Shen, Z.; Zhao, W. *J. Mol. Struct.* **1996**, *375*, 95.

(32) Huber, K. P.; Herzberg, G. *Molecular Spectra and Molecular Structure. IV. Constants of Diatomic Molecules*; van Nostrand Reinhold: New York, 1979.

(33) Larzillière, M.; Jacox, M. E. *J. Mol. Spectrosc.* **1980**, *79*, 132.

(339) ν_2 (a'), 645.8 (20) ν_3 (a'), 377.3 (28) ν_4 (a'), 235.3 (6) ν_5 (a'), 207.6 (1) ν_6 (a'').

The energies, geometries, and $\nu(\text{MP})$ stretching frequencies were calculated for both the singlet and triplet states of the diatomic MP molecule. The triplet species are lower in energy, the difference between the singlet and triplet states being 109.8, 85.7, and 95.1 kJ mol⁻¹ for M = Al, Ga, and In, respectively. Thus, MP molecules follow the same trend as do MN molecules.³⁴ The bond lengths (in Å) are 1.7995, 2.2616, and 2.4662 for the singlet and 1.6809, 2.1018, and 2.2838 for the triplet states of MP (with M = Al, Ga, and In, respectively). The corresponding $\nu(\text{M}-\text{P})$ modes occur at 744.3 (7), 345.7 (15), 280.2 (8) and 938.2 (4), 431.8 (5), 365.1 (1) cm⁻¹ (with the IR intensities in km mol⁻¹ in parentheses). The experimental value of 283.6 cm⁻¹ for ⁶⁹GaP³⁵ is in good agreement with our theoretical results.

Stereochemistry and Bonding. It comes as no surprise that the ground states of the HMPH₂, H₂MPH₂, and MPH₂ molecules each have an absolute energy minimum with a nonplanar MPH₂ unit, in contrast to the planar forms of the corresponding nitrogen compounds.⁹ However, theoretical studies show that compounds containing planar tricoordinated phosphorus are good π -type electron-pair donors. π -Electron-pair acceptors should therefore stabilize the planar structure, and indeed, calculations predict planar structures for H₂CPH₂⁺ and HCPH₂.^{36,37} In pseudoaromatic systems, too, tricoordinated phosphorus can be found in a trigonal planar environment, e.g., 1-[bis(trimethylsilyl)methyl]-3,5-bis(trimethylsilyl)-1,2,4-triphosphole, the nucleus of which is a planar five-membered ring.³⁸

For PH₃ we derive a value of 148.2 kJ mol⁻¹ for the barrier to inversion, in excellent agreement with earlier estimates (146.8,³⁹ 145.8,⁴⁰ and 143.9 kJ mol⁻¹⁴¹), although the value determined experimentally⁴² is somewhat lower (132 kJ mol⁻¹). The energies for planarization of the HMPH₂ compounds are calculated to be 42.6, 56.7, and 59.2 kJ mol⁻¹ for M = Al, Ga, and In, respectively. Thus, the replacement of an H atom by an HM group with the potential to act as a π -type acceptor lowers significantly the barrier to inversion. The M-P-M-H bond lengths decrease from 2.3713/1.6065, 2.3919/1.6117, and 2.6031/1.7762 Å for the appropriate molecule in its lowest energy conformation (*C*₁ symmetry) to 2.2434/1.5936, 2.2505/1.5876, and 2.4498/1.7527 Å for the planar conformation (*C*_s symmetry), wherein the Ga-H bond is slightly shorter than the Al-H bond. The H-P-H/H-M-P angles change from 94.9/114.4°, 94.3/115.4°, and 93.8/115.3° for the nonplanar structure to 106.0/115.0°, 106.4/117.4°, and 105.3/115.5° for the planar one.

Our calculations find also nonplanar energy minima for the compounds H₂MPH. However, the energy difference between the nonplanar and the planar structures is insignificant, amount-

ing to only 0.13, 0.87, and 0.11 kJ mol⁻¹ for M = Al, Ga, and In, respectively. In previous calculations by Davy and Schaefer,²⁵ the planar form of H₂AlPH emerges as the minimum energy configuration. Rotation about the M-P bond starting from the planar geometry is met by a barrier of 1.61, 0.03, and 1.20 kJ mol⁻¹ for Al, Ga, and In, respectively. The results of the calculations thus suggest that the degree of π -interaction in the H₂MPH species is negligible. The effect of planarization on the bond lengths is, as expected, minimal. Thus, the M-P bond lengths change from 2.3523, 2.3421, and 2.5554 Å to 2.3569, 2.3539, and 2.5596 Å in the planar form and to 2.3469, 2.3394, and 2.5506 Å after subsequent 90° rotation about the M-P bond.

Reaction Mechanisms. The reactions of Al, Ga, or In atoms with PH₃ differ notably from the reactions with NH₃.⁹ Like the corresponding ammonia adducts, the phosphine adducts M·PH₃ tautomerize on photolysis at wavelengths near 436 nm to give the insertion product HMPH₂. However, in the case of the reactions with PH₃, the IR spectra also disclose the formation of H₂MPH at this stage; the corresponding species H₂MNH are not observed.⁹ The phosphine experiments indicate that HMPH₂ and H₂MPH are formed independently with M·PH₃ being the precursor to both. The theoretical investigations show that the divalent HMPH₂ and the trivalent H₂MPH are very close in energy, thereby lending strong support to the conclusion that both are generated together on photolysis at $\lambda = 436$ nm. Accordingly, the IR absorptions due to the adduct M·PH₃ decay while those due to HMPH₂ and H₂MPH are observed to grow. The calculations predict an increasing energy difference between HMPH₂ and H₂MPH in the order Al < Ga < In, so the HMPH₂ isomer is favored by the heavier group 13 elements (see Scheme 1). The progressive dominance of the absorptions of HMPH₂, starting from a roughly 1:1 mixture of HMPH₂ and H₂MPH in the case of Al and moving to a situation in which little H₂MPH can be detected in the case of In, reflects this trend and gives additional support to our interpretation of the spectra.

For the reactions with Al, no photoproduct other than HAIPH₂ and H₂AlPH is observed. In the case of Ga and In, however, PH is additionally formed. HMPH₂ appears the most likely precursor to this product. The decomposition of HMPH₂ on further photolysis leads to a growth of the PH absorption. There is, on the other hand, no evidence for any buildup of PH in the last photolysis step, where H₂MPH is decomposed by photolysis with UV radiation (200 ≤ λ ≤ 400 nm). The route from HMPH₂ to PH involves the rupture of the M-P bond. The Al-P bond is stronger than the Ga-P or In-P bond, and so it is reasonable that only HGaPH₂ and HInPH₂ should follow this route. One possible mechanism is the elimination of dihydrogen resulting in the formation of an intermediate MPH, which then undergoes dissociation to the metal atoms and PH.

The UV-vis spectra give clear evidence of an absorption maximum near 550 nm associated with HAIPH₂. Photolysis into this absorption leads to the decomposition of HAIPH₂, and similar behavior was observed on the parts of HGaPH₂ and HInPH₂. While HMPH₂ decays on photolysis at $\lambda = 546$ nm, its isomer H₂MPH persists. The IR signal due to PH increases slightly but significantly. Moreover, the IR spectra give clear evidence for a partial recovery of the adduct M·PH₃. Thus, the decomposition of HMPH₂ under these conditions proceeds via at least two channels for M = Ga and In.

H₂MPH and, in the case of Ga and In, PH are left after photolysis at $\lambda = 546$ nm. Both species are also resistant to photolysis with radiation at $\lambda \geq 450$ nm, thus indicating that H₂MPH has no destructive absorption maximum in the visible region. However, photolysis with UV light (200 ≤ λ ≤ 400

(34) Andrews, L.; Zhou, M.; Chertihin, G. V.; Bare, W. D.; Hannachi, Y. *J. Phys. Chem. A* **2000**, *104*, 1656. Zhou, M.; Andrews, L. *J. Phys. Chem. A* **2000**, *104*, 1648.

(35) Li, S.; Van Zee, R. J.; Weltner, W., Jr. *J. Phys. Chem.* **1993**, *97*, 11393.

(36) Schade, C.; Schleyer, P. v. R. *J. Chem. Soc., Chem. Commun.* **1987**, 1399.

(37) Kapp, J.; Schade, C.; El-Nahasa, A. M.; Schleyer, P. v. R. *Angew. Chem., Int. Ed. Engl.* **1996**, *35*, 2236.

(38) Cloke, F. G. N.; Hitchcock, P. B.; Hunnabell, P.; Nixon, J. F.; Nyulászi, L.; Niecke, E.; Thelen, V. *Angew. Chem., Int. Ed. Engl.* **1998**, *37*, 1083.

(39) Schwerdtfeger, P.; Laakkonen, L. J.; Pyykkö, P. *J. Chem. Phys.* **1992**, *96*, 6807.

(40) Ahlrichs, R.; Keil, F.; Lischka, H.; Kutzelnigg, W.; Staemmler, V. *J. Chem. Phys.* **1975**, *63*, 455.

(41) Marynick, D. S.; Dixon, D. A. *J. Phys. Chem.* **1982**, *86*, 914.

(42) Weston, R. E., Jr. *J. Am. Chem. Soc.* **1954**, *76*, 2645.

nm) initiates rapid decomposition of H_2MPH . The signal due to PH does not gain intensity at this stage, so PH is unlikely to be a decomposition product of H_2MPH . There is no evidence either that the $\text{M}\cdot\text{PH}_3$ adduct is regenerated. Moreover, the UV-vis spectra give no indication of significant recovery of free metal atoms, although the information level is limited by band-broadening, so small changes of concentration would probably escape notice. Photolysis at $\lambda = 436$ nm after a period of broad-band photolysis fails also to deliver any sign of the signals due to HMPH_2 or H_2MPH . Hence, we are bound to conclude that another product, e.g., MP, is an ultimate destination of the reactions. Unfortunately, the low IR intensity of the vibrational fundamental of this molecule then frustrates its detection.

Conclusions

The thermal and photochemical reactions that occur between the group 13 metal atoms Al, Ga, and In and PH_3 have been investigated by matrix-isolation experiments, the course of events being tracked and the various products being identified and characterized primarily by their IR spectra but in some cases also by their visible spectra. The analysis has been underpinned crucially (i) by the response of the IR spectra to replacing PH_3 by PD_3 and (ii) by the guidance of the vibrational properties simulated by DFT calculations for a variety of individual molecules.

The first product formed by the thermal reaction of the metal atoms with PH_3 is the adduct $\text{M}\cdot\text{PH}_3$ ($\text{M} = \text{Al, Ga, or In}$). Although no distinctive visible absorption band could be detected (cf. $\text{M}\cdot\text{NH}_3$, which absorbs near 428 nm^9), this species is photolabile at wavelengths in the range $400\text{--}450\text{ nm}$. The divalent species HMPH_2 and the trivalent one H_2MPH are the products formed following photolysis of the adducts at $\lambda = 400\text{--}450\text{ nm}$. In the experiments with Ga and In, PH is additionally formed, probably from HMPH_2 . HMPH_2 was also characterized by a visible absorption band near 550 nm ,

irradiation into which results in decomposition of the molecule and partial recovery of the adduct $\text{M}\cdot\text{PH}_3$. A second channel, open only to the Ga and In species, involves decomposition to give PH (together presumably with dihydrogen and metal atoms). H_2MPH is destroyed by UV radiation ($200 \leq \lambda \leq 400\text{ nm}$) without the emergence of a metal-containing product identifiable by its IR or UV-vis spectrum. At the end, the only detectable reaction product is PH.

The reactions of the group 13 metal atoms Al, Ga, and In with PH_3 thus differ appreciably from the previously investigated reactions with NH_3 .⁹ In the case of NH_3 , photolysis of the adducts at $\lambda = 436\text{ nm}$ gives the single product HMNH_2 ; there is no evidence for the isomer H_2MNH , which is a high-energy species according to previous theoretical investigations.²⁹ Instead, the trivalent and univalent derivatives, H_2MNH_2 and MNH_2 , respectively, are formed when HMNH_2 decomposes under the action of broad-band UV-visible radiation.⁹

The properties of the compounds $\text{M}\cdot\text{PH}_3$, HMPH_2 , and H_2MPH anticipated by the DFT calculations are compared with those (i) of the known or hypothetical molecules H_2MPH_2 , MPH_2 , HMPH , and MP , and (ii) of analogous species derived from NH_3 .⁹ Unlike the corresponding amides, HMPH_2 features a pyramidal $\text{M}\text{--}\text{PH}_2$ moiety. A fuller discussion of the bonding and other properties of compounds featuring $\text{M}\text{--}\text{N}$ or $\text{M}\text{--}\text{P}$ bonds (where M is a group 13 metal atom) will be found elsewhere.⁴³

Acknowledgment. The authors thank (i) the EPSRC for support of this research, including the purchase of equipment and the award of an Advanced Fellowship to T.M.G. and (ii) the Deutsche Forschungsgemeinschaft for the award of a postdoctoral grant to H.-J.H.

IC000837V

(43) Himmel, H.-J.; Downs, A. J.; Greene, T. M. *J. Chem. Soc., Dalton Trans.*, in press.